CHAPTER IV
RESULTS AND DISCUSSIONS

4.1 Catalyst Screening

A mass spectrometer (MS) was used for qualitative analysis of product gas. The possible products are listed in Table 4.1. The chemical assignments have been done and agreed with other assignments reported in other literatures (Shen *et al.*, 2003) Hydrogen and ethylene were selected to evaluate generated inorganic and olefins, respectively. Figures 4.1, 4.2, 4.3 and 4.4 present possible mass of hydrogen, carbon monoxide, methane and ethylene, respectively.

Table 4.1 Selected molecular ions from mass spectrometer

m/z ratio	Molecular ions	Mainly due to
2	H_2+	Hydrogen
15	CH_3+	Methane
26	C_2H_2+	Ethylene
28	CO+	Carbon monoxide
30	C_2H_6+	Ethane
39	C_3H_3+	Propylene
42	C_3H_8+	Propane
44	CO_2+	Carbon dioxide

Hydrogen evolved in the wide range of temperature (400-900 °C). Carbon monoxide evolved first in the range of temperature 300-500 °C and will be increased over 600 °C. The evolution profiles of Methane slightly change but it declined at high temperature.

Ethylene evolved first at temperature between 200-400 °C for all samples. Then, ethylene dominated again at temperature between 700-900 °C. At constant

temperature section (900 °C) ethylene and hydrogen intensities decreased due to the depletion of cellulose in reactor.

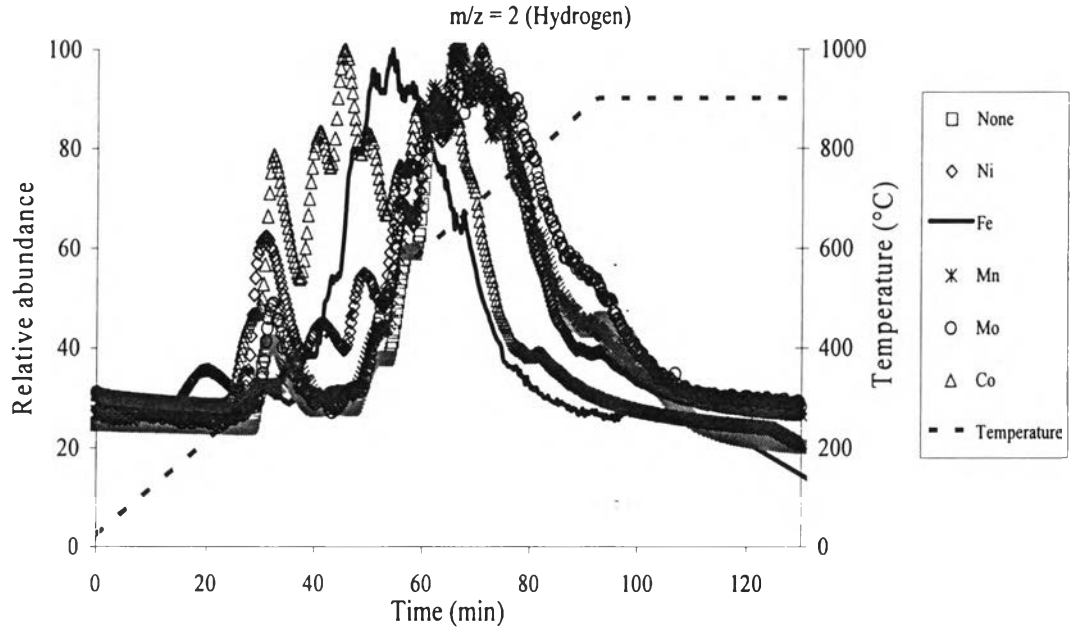

Figure 4.1 Evolution profiles of hydrogen from CO_2 gasification of cellulose with different catalysts : (□) none, (-) Fe, (Δ) Co, (◊) Ni, (*) Mn, (○) Mo, and (--) temperature.

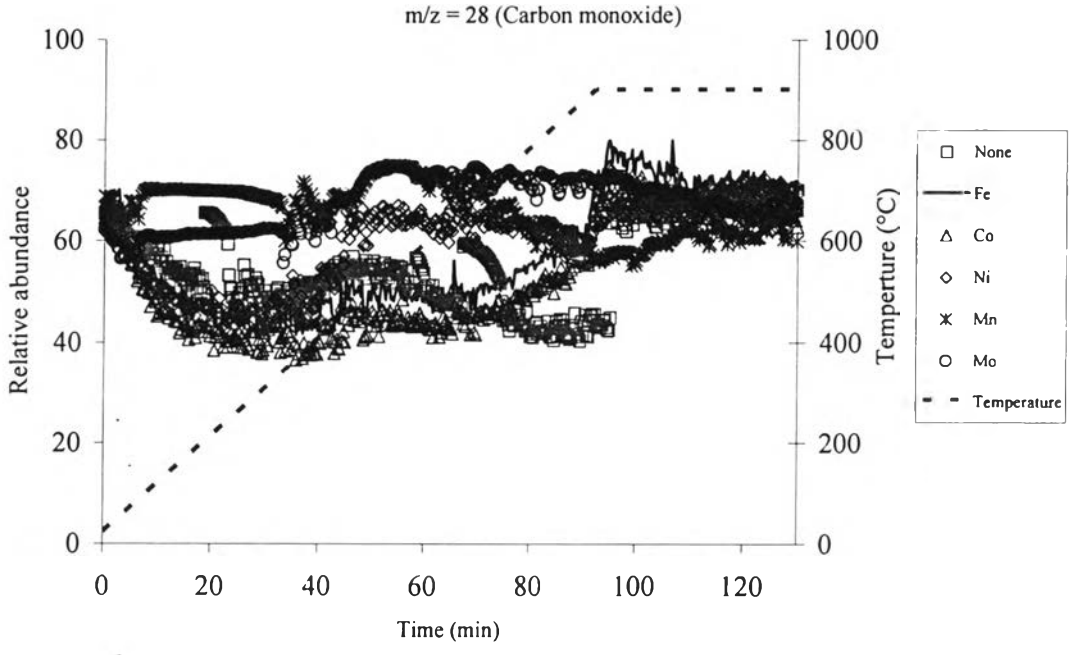

Figure 4.2 Evolution profiles of carbon monoxide from CO_2 gasification of cellulose with different catalyst : (□) none, (-) Fe, (Δ) Co, (◊) Ni, (*) Mn, (○) Mo, and (--) temperature.

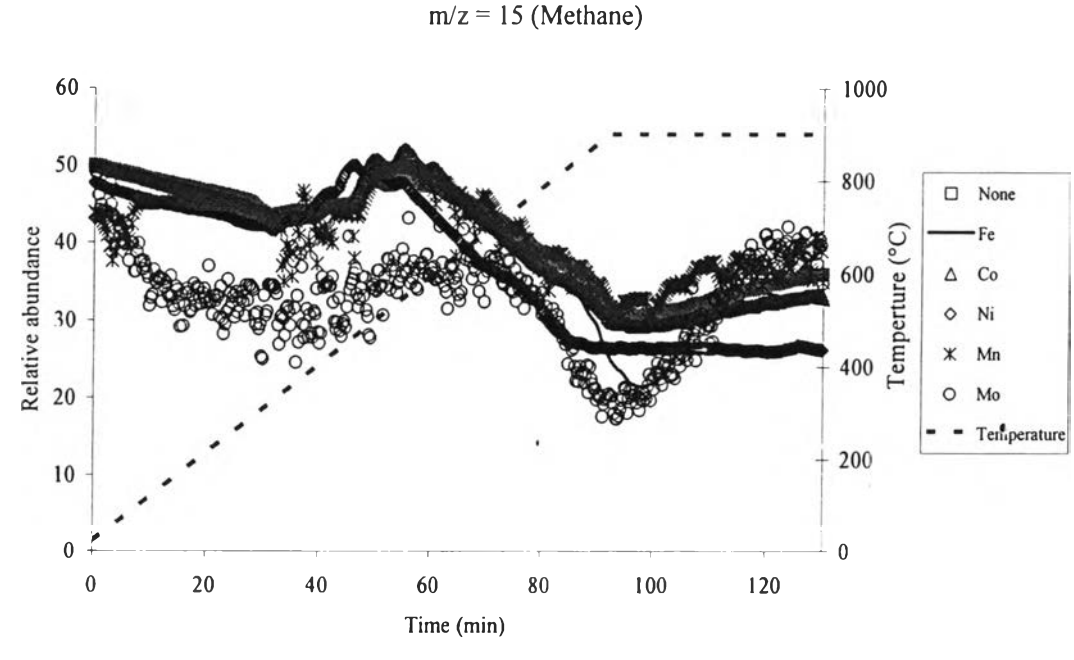

Figure 4.3 Evolution profiles of methane from CO_2 gasification of cellulose with different catalyst : (□) none, (-) Fe, (Δ) Co, (◊) Ni, (*) Mn, (○) Mo (--) temperature.

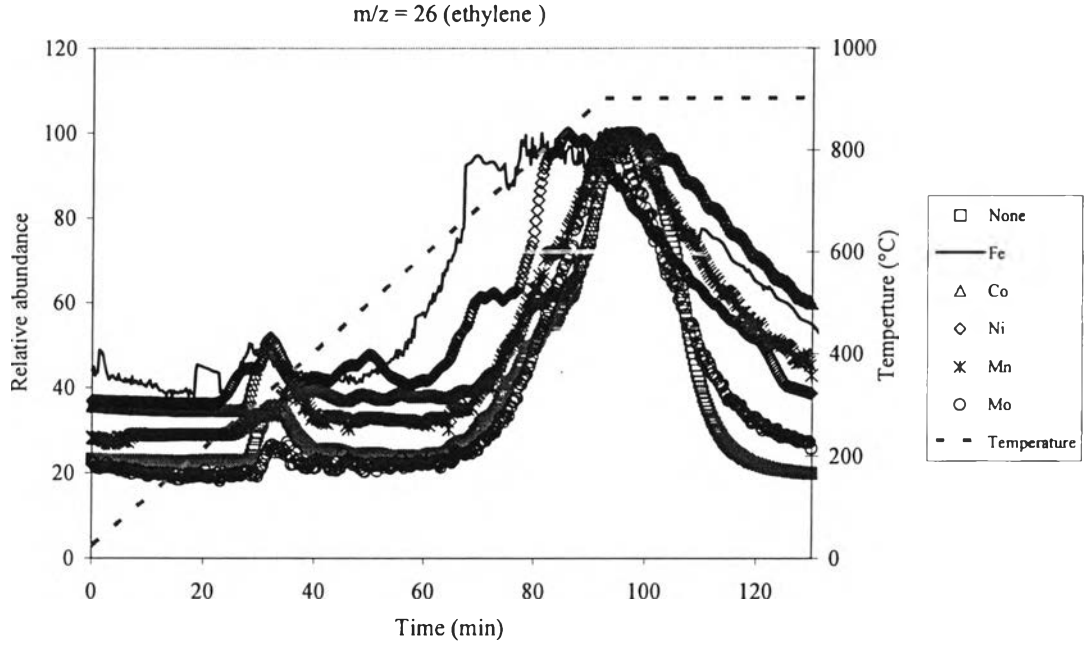

Figure 4.4 Evolution profiles of ethylene from CO_2 gasification of cellulose with different catalyst : (□) none, (-) Fe, (Δ) Co, (◊) Ni, (*) Mn, (○) Mo (--) temperature.

Table 4.2 Integrated MS intensities (arbitrary units)

Catalyst	None	Fe	Co	Ni	Mn	Mo
H_2	2261	3206	3114	**3442**	2688	2547
CO	3366	3705	3643	3629	3430	3596
CH_4	1411	1563	1486	1484	1430	1574
C_2H_4	2363	**2971**	**2850**	2516	2436	2478

To identify the possible catalyst, the mass spectrum intensity was integrated to obtain the peak area. The peak area of ethylene and hydrogen are used for identification the possible catalyst. The results show that the peak area of ethylene was high in case of Fe and Co catalyst. Ni catalyst shows the highest intensity of Hydrogen. Mn and Mo have similar tendency but their H_2 and C_2H_4 intensities are lower than Co, Fe and Ni. Hence, Co and Fe were selected as catalysts in this study.

4.2 Catalyst Characterization

4.2.1 BET Surface Area

The selected catalysts (Fe and Co), the synthesized Co-Fe and ZSM-5 were measured their surfaces areas by the multiple point BET method. The BET surface areas of Fe, Co, Co-Fe and ZSM-5 are reported in Table 4.3. The BET surface areas of Fe, Co and Co-Fe catalysts are low due to the aggregation of metal particle during the precipitation of catalyst preparation. This leads to the decrease of pore volume and surface area. The SEM pictures of fresh catalysts show the aggregation of particle in Figures 4.5, 4.6 and 4.7.

Table 4.3 BET surface areas of prepared catalyst

Catalyst	BET surface area (m^2/g)
Co	2.92
Fe	2.97
Co-Fe	2.88
ZSM-5	360

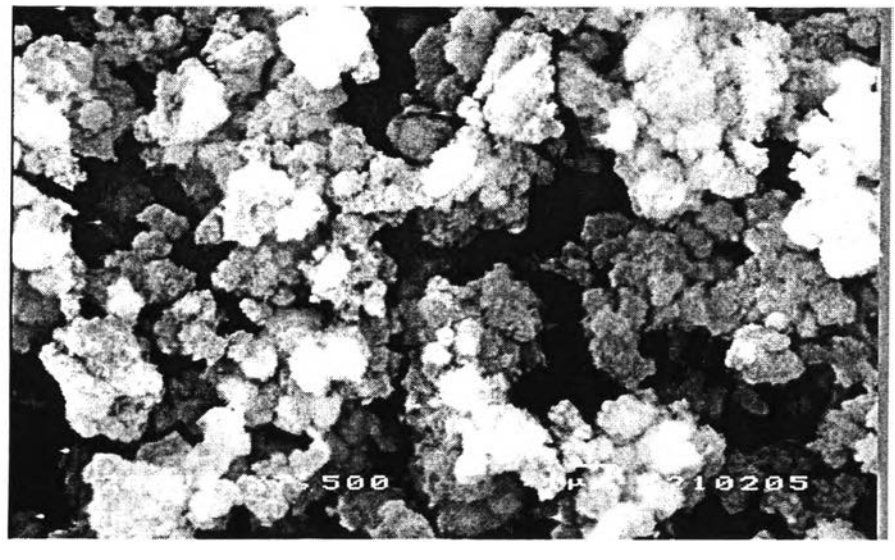

Figure 4.5 SEM picture of fresh Co catalyst.

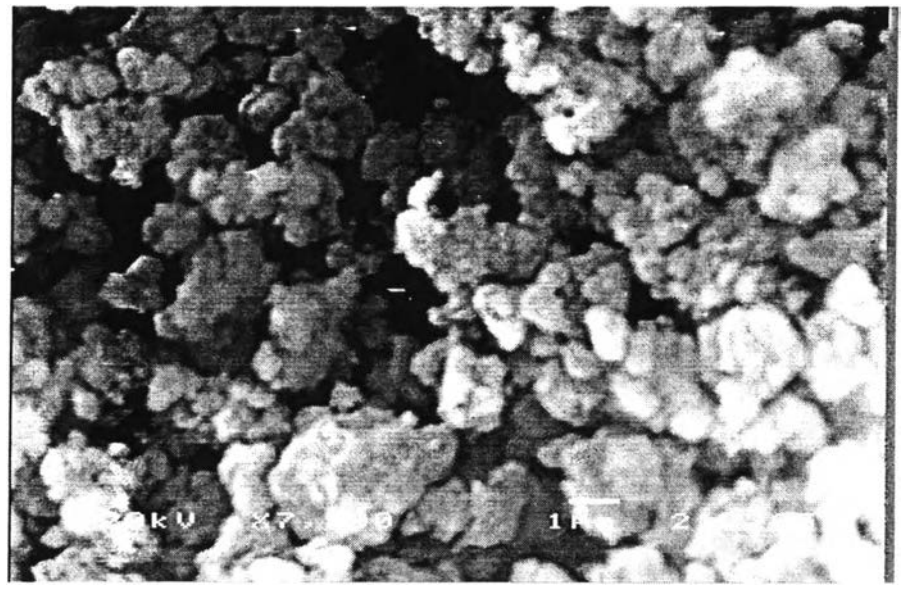

Figure 4.6 SEM picture of fresh Fe catalyst.

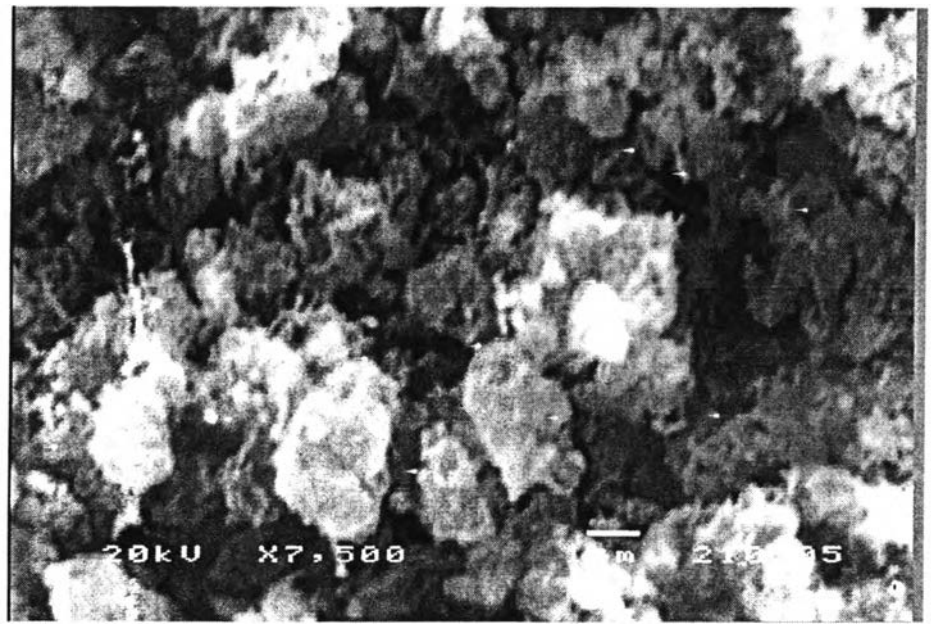

Figure 4.7 SEM picture of fresh Co-Fe catalyst.

4.2.2 X-Ray Diffraction (XRD)

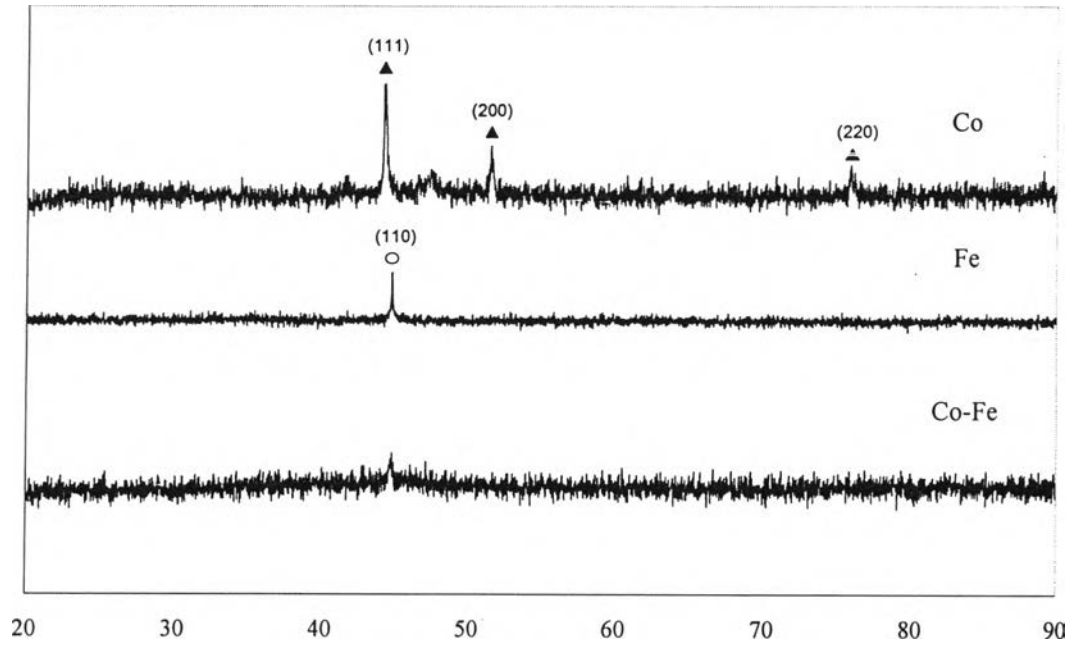

Figure 4.8 XRD patterns of fresh Co, Fe, and Co-Fe catalysts : (▲) Co and, (○) Fe.

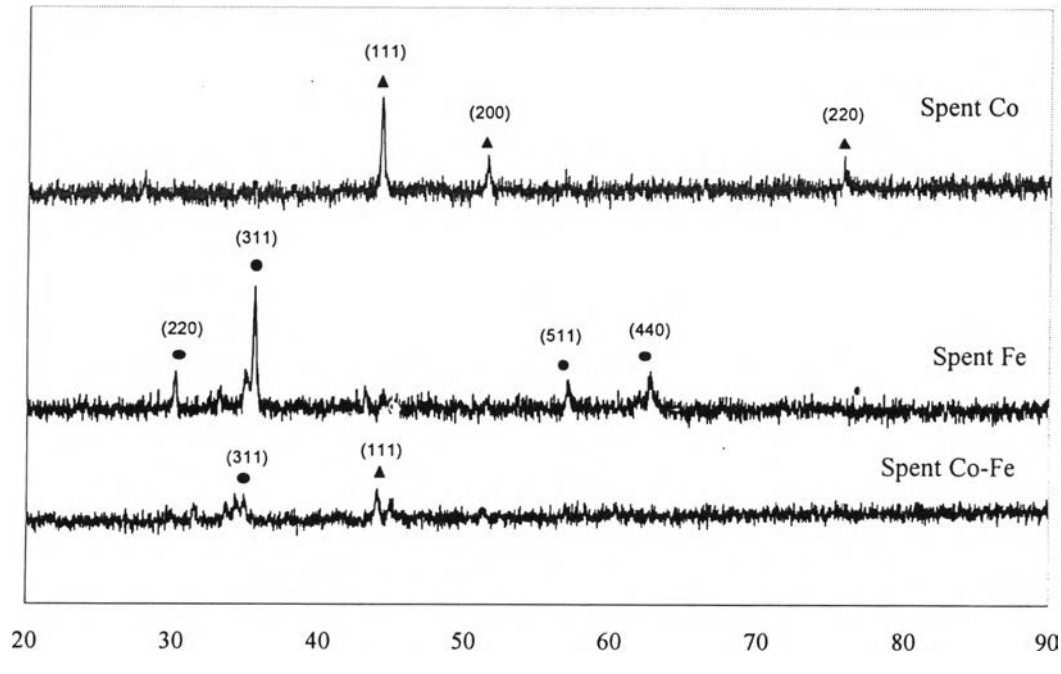

Figure 4.9 XRD patterns of spent Co, Fe, and Co-Fe catalysts from CO_2 gasification of cellulose : (●) Fe_2O_3-magnetite, and (▲) Co.

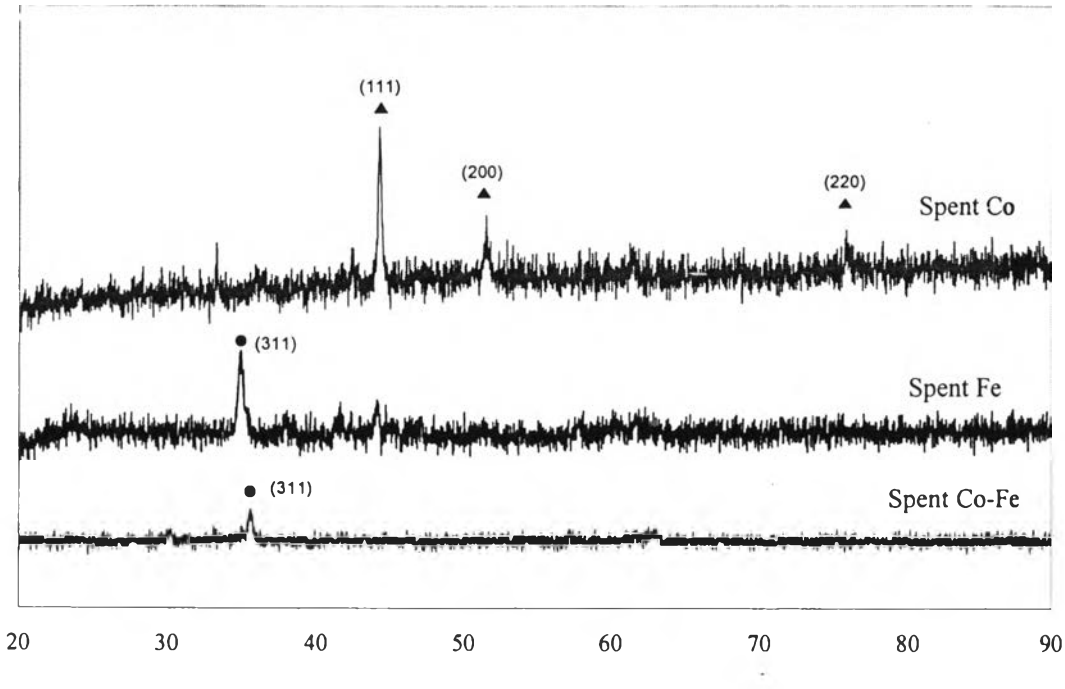

Figure 4.10 XRD patterns of spent Co, Fe, and Co-Fe catalysts from steam gasification of cellulose : (●) Fe_2O_3-magnetite, and (▲) Co.

Table 4.4 Crystal size of fresh and spent catalyst

Crystal size of catalyst at different condition (nm)			
Catalyst	**Fe**	**Co**	**Co-Fe**
Fresh	16.21	19.26	19.19
Spent with CO_2 at 700 °C	28.90	27.37	23.05
Spent with steam at 700 °C	20.38	29.71	22.32

XRD analysis was carried out for Co, Fe and Co-Fe catalyst. The results show that there exist Co phase in fresh Co catalyst. Three main characteristic peaks for Co at 2θ = 44.3°, 51.5° ,and 76.1° related to the (111), (200) and (220) planes and revealed that the resultant particles were pure metallic Co with a face-cntered cubic (FCC) structure. In the case of fresh Fe, the preferentially oriented crystal plane is found to be (110). On the other hand, there is very low existence of crystalline phase in Co-Fe catalyst. This reveals that the prepared Co-Fe catalyst maybe formed in amorphous phase.

The XRD patterns of spent catalysts from CO_2 gasification and steam gasification are shown in Figures 4.9 and 4.10, respectively. The results show that

there exist Fe_2O_3 – magnetite phase in spent Fe catalyst from both of CO_2 gasification and steam gasification. The preferentially oriented crystal plane of magnetite is found to be (311). This could be suggested that Fe phase in Fe catalyst change to magnetite phase due to the oxidation reaction with steam or CO_2. On the other hand, the XRD pattern for spent Co catalyst showed three main characteristic peaks for Co ($2\theta = 44.3°$, $51.5°$,and $76.1°$), marked by their indices ((111), (200) and (220)), were observed. This suggested that Co catalyst is stable under reactive atmosphere of CO_2 or steam.

The fresh Co-Fe catalyst showed an amorphous phase. After gasification reaction, there magnetite phase ((311)) exists in spent Co-Fe catalyst. This could be suggested that Co-Fe bimetallic catalyst mainly consisted of Fe phase and Co phase highly dispersed in Fe structure.

The crystal size of spent catalysts is bigger than their fresh state. This could be due to the agglomeration of metal particle to form a bigger particle at high temperature.

4.3 Gasification of Cellulose

The gasification of cellulose was carried out through diferrent experimental series by varying temperature (600-800 °C), gasifying agents and catalysts. The catalyst are Fe, Co, Co-Fe and pure cellulose were tested for catalytic and non-catalytic gasification, respectively. In addition, the commercial ZSM-5 catalyst was also tested for comparison with prepared catalysts. The gasifying agents are pure CO_2 and pure steam. The ratio of catalyst to cellulose for all tests was 1:5 by weight.

4.3.1 Product Distribution from CO_2 Gasification

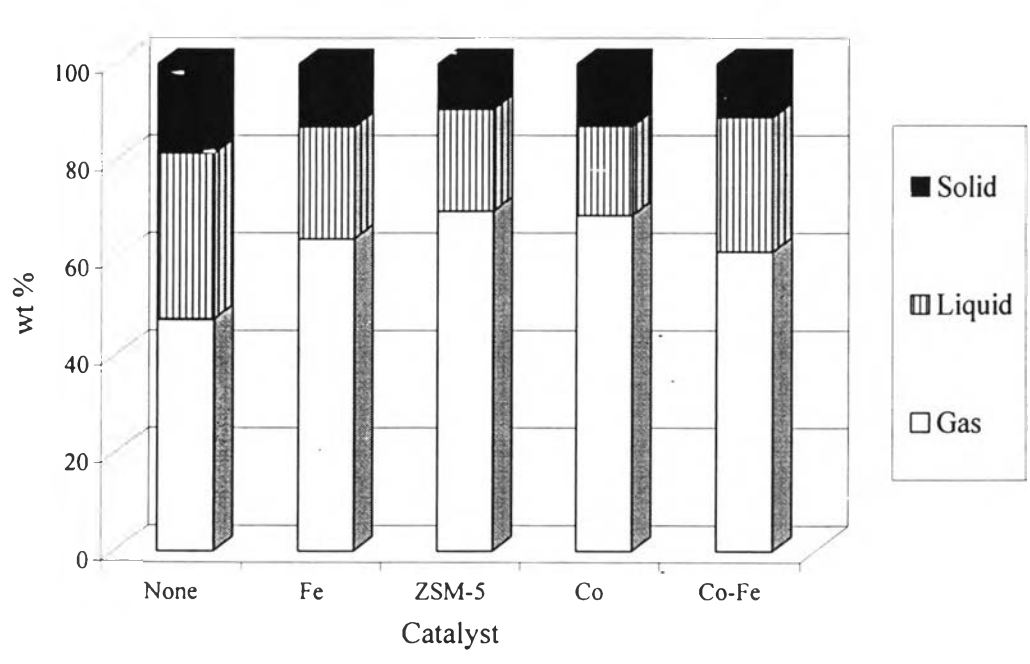

Figure 4.11 Product distribution from CO_2 gasification at 600 °C.

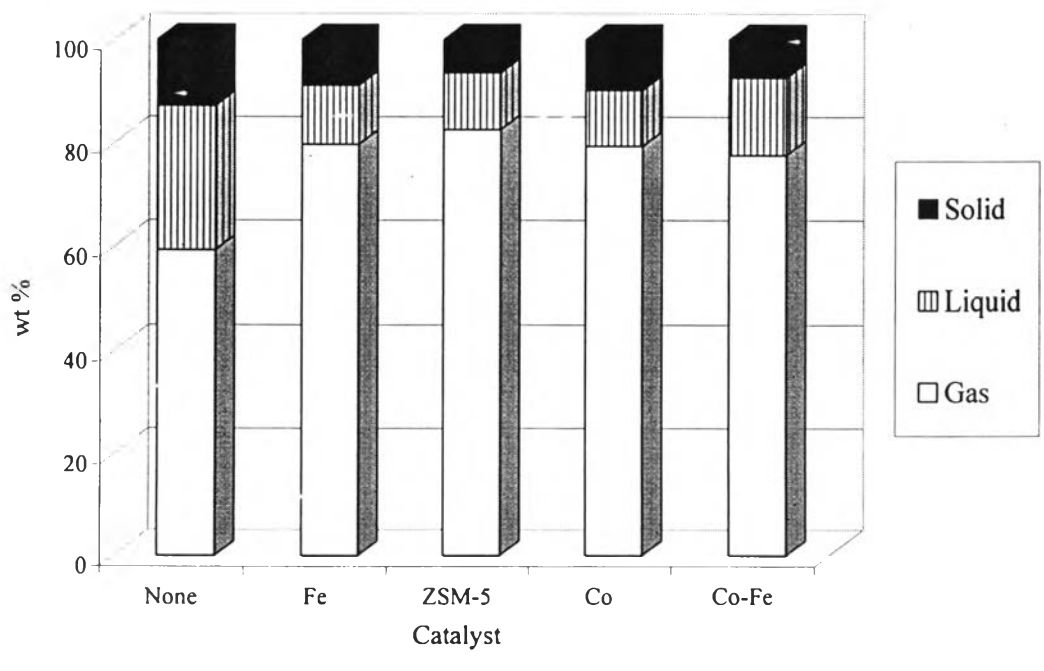

Figure 4.12 Product distribution from CO_2 gasification at 700 °C.

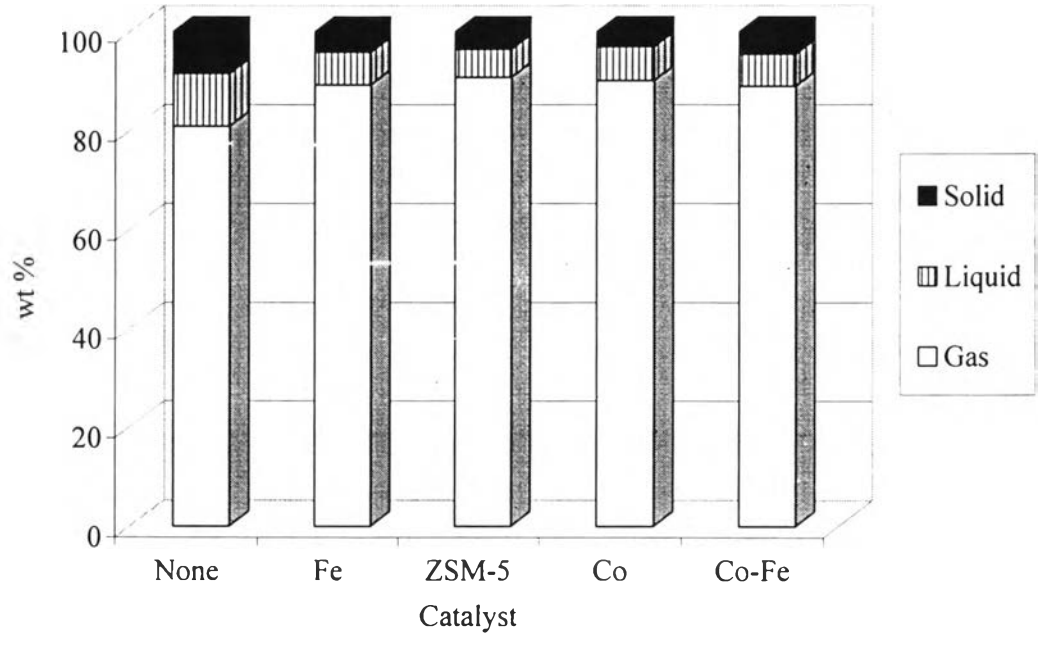

Figure 4.13 Product distribution from CO_2 gasification at 800 °C.

The product distribution of CO_2 gasification at 600, 700 and 800 °C were presented in Figures 4.11, 4.12 and 4.13, respectively. As observed, gas yield increased with increasing gasifying temperature, meanwhile liquid and solid yield are necessarily decreased. The decrease of liquid fraction due to the liquid cracking with the increasing temperature, which yields an increase in gas formation. This could be explained by the growing importance of gasification with respect to pyrolysis when temperature increases. As a consequence, a major gaseous product is obtained.

4.3.2 Gas Production from CO_2 Gasification

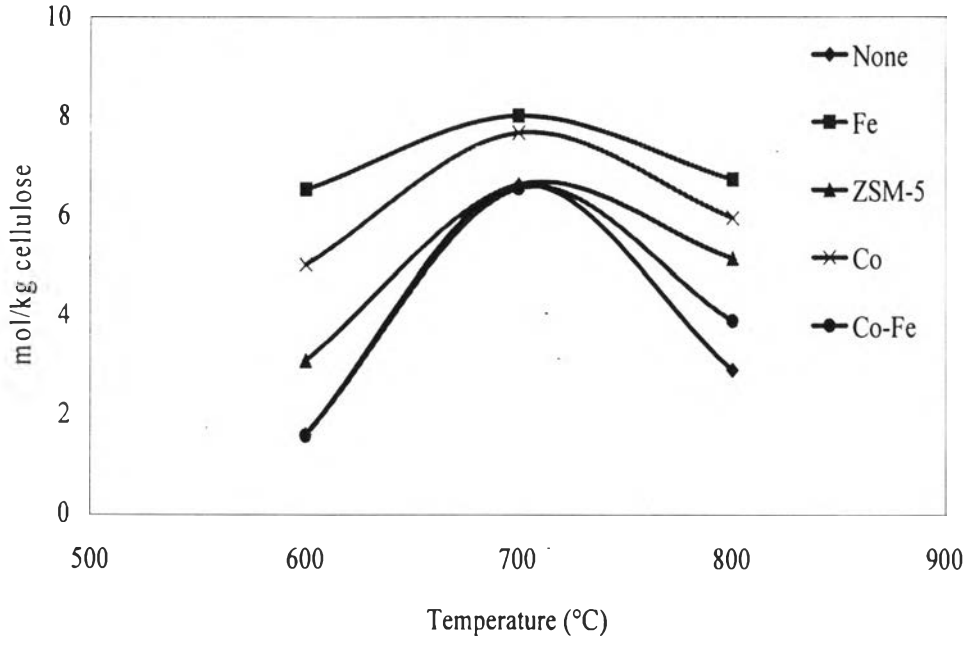

Figure 4.14 H_2 production from CO_2 gasification with and without catalysts : (♦) None, (▲) ZSM-5, (■) Fe, (x) Co, and (●) Co-Fe.

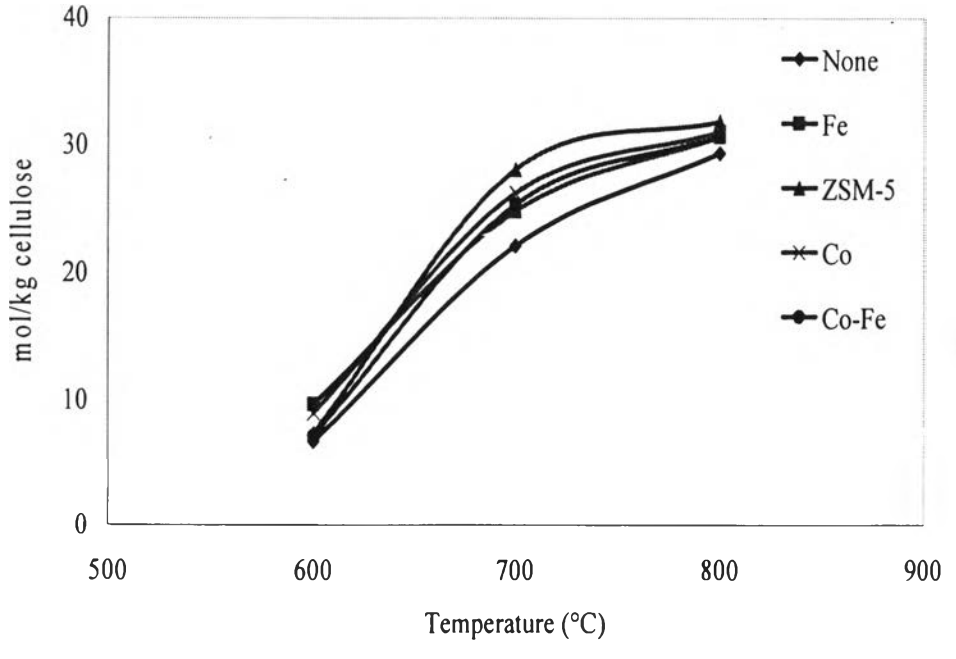

Figure 4.15 CO production from CO_2 gasification with and without catalysts : (♦) None, (▲) ZSM-5, (■) Fe, (x) Co, and (●) Co-Fe.

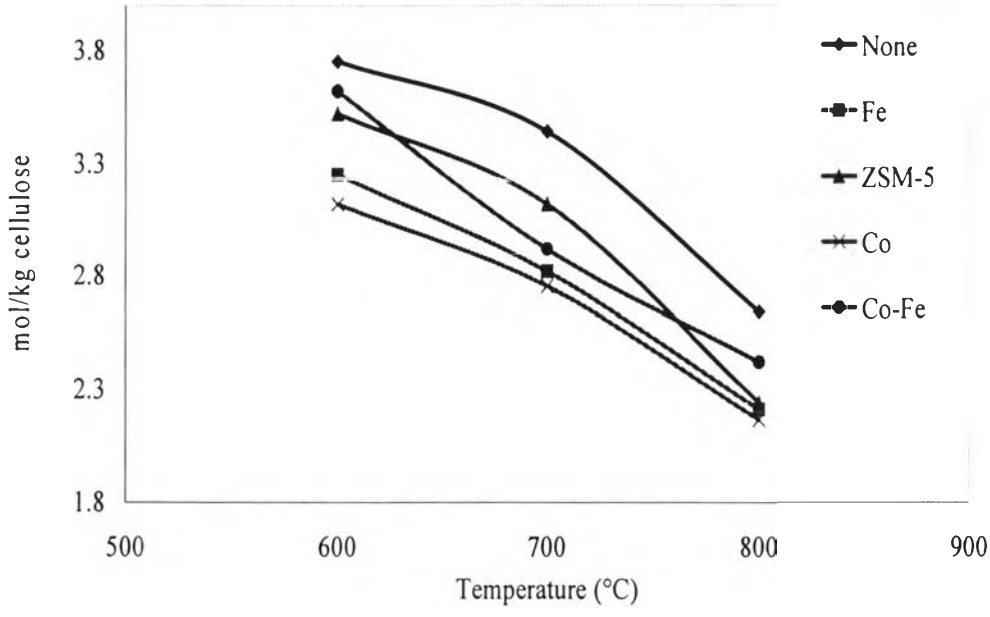

Figure 4.16 CH_4 production from CO_2 gasification with and without catalysts : (♦) None, (▲) ZSM-5, (■) Fe, (x) Co, and (●) Co-Fe.

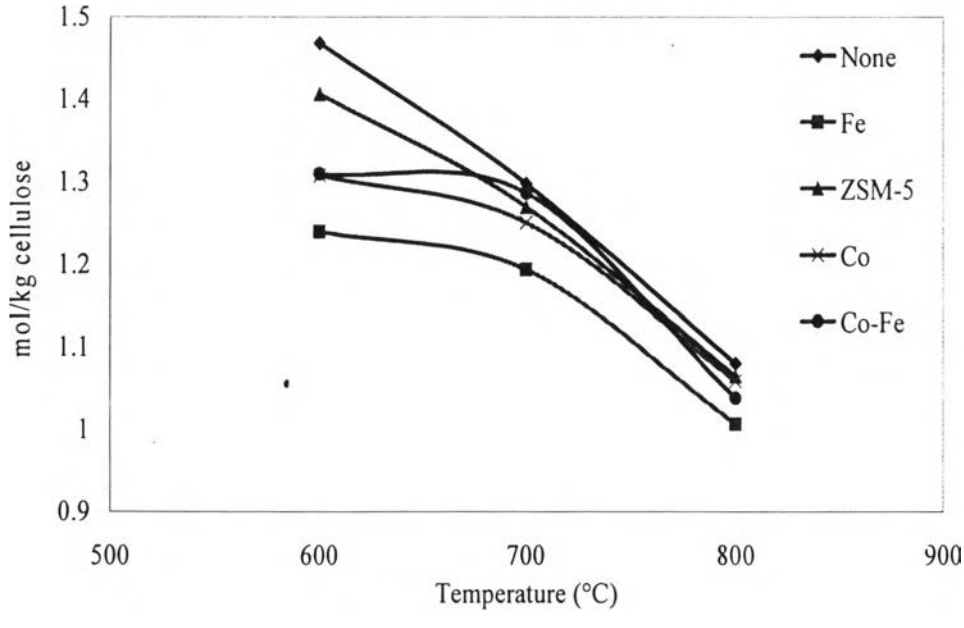

Figure 4.17 C_2H_4 production from CO_2 gasification with and without catalysts : (♦) None, (▲) ZSM-5, (■) Fe, (x) Co, and (●) Co-Fe.

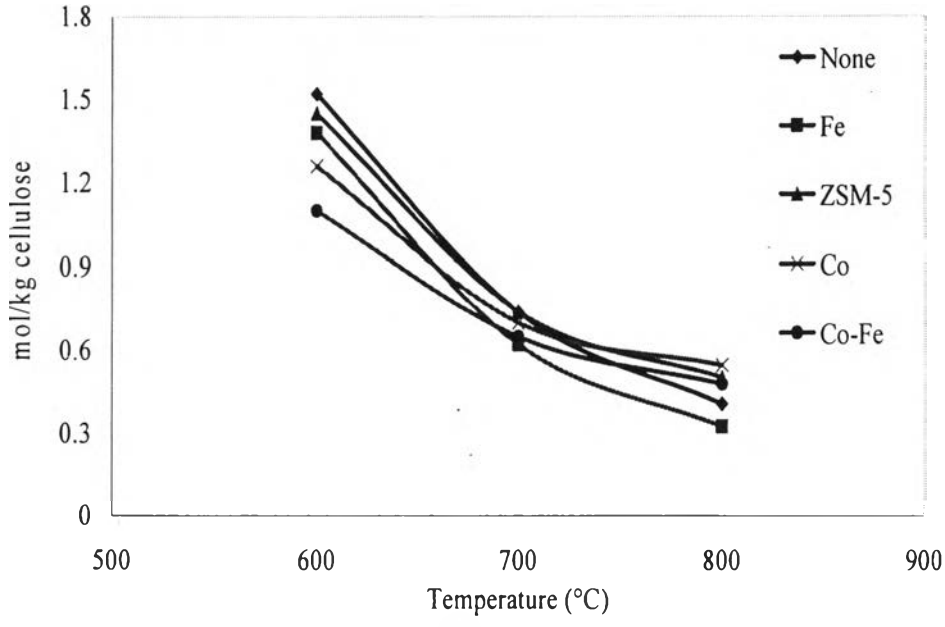

Figure 4.18 C_2H_6 production from CO_2 gasification with and without catalysts : (♦) None, (▲) ZSM-5, (■) Fe, (x) Co, and (●) Co-Fe.

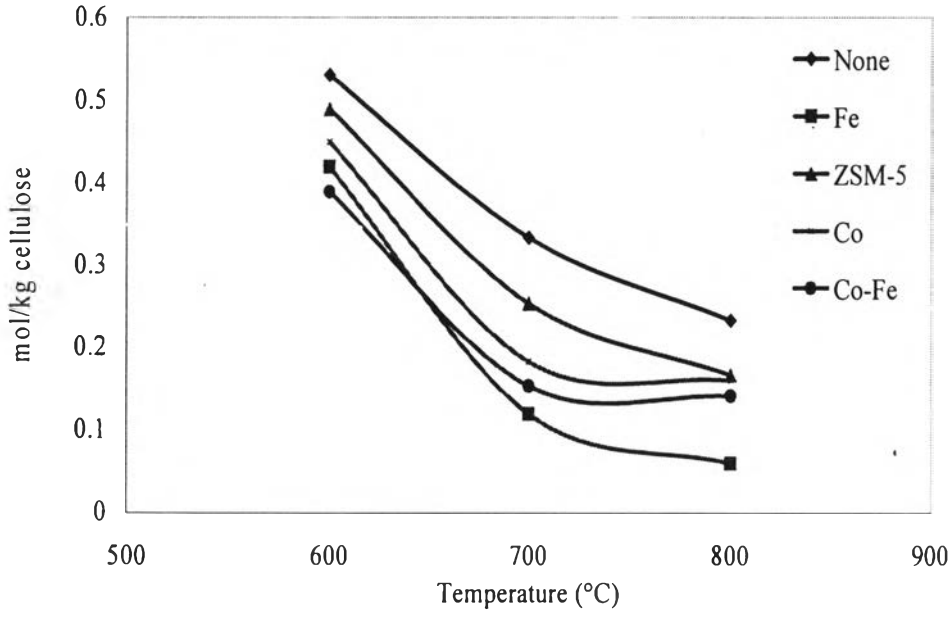

Figure 4.19 C_3H_8 production from CO_2 gasification with and without catalysts : (♦) None, (▲) ZSM-5, (■) Fe, (x) Co, and (●) Co-Fe.

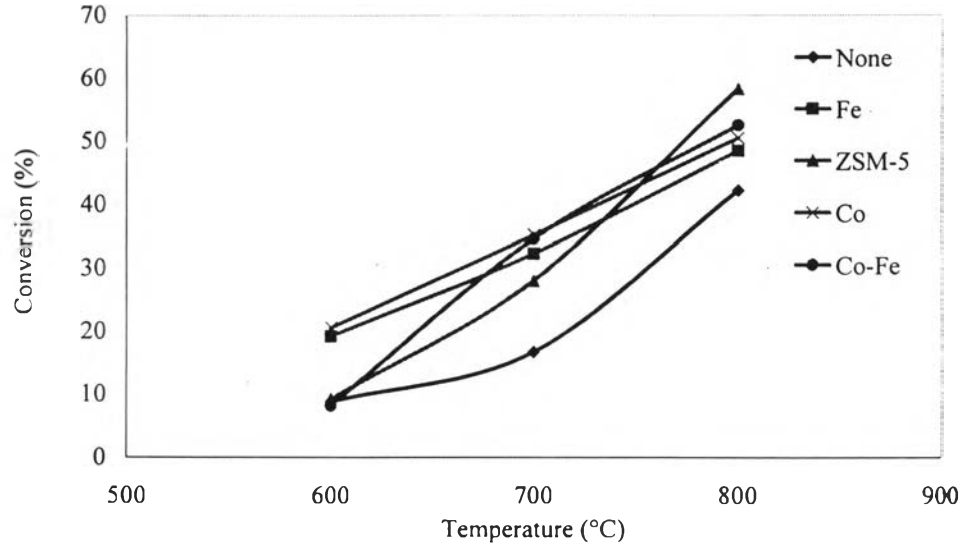

Figure 4.20 CO_2 conversion from CO_2 gasification with and without catalysts : (♦) None, (▲) ZSM-5, (■) Fe, (x) Co, and (●) Co-Fe.

The gas production of H_2, CO, CH_4, C_2H_4, C_2H_6, C_3H_8 and CO_2 conversion are presented in Figures 4.14, 4.15, 4.16, 4.17, 4.18, 4.19 and 4.20, respectively.

$$C_nH_x + CO_2 \rightarrow (x/2)H_2 + 2nCO \quad (1)$$

$$CH_4 + CO_2 \leftrightarrow 2H_2 + 2CO \quad (2)$$

$$C_2H_4 + 2CO_2 \leftrightarrow 2H_2 + 4CO \quad (3)$$

$$CO_2 + H_2 \leftrightarrow CO + H_2O \quad (4)$$

$$CO + H_2O \leftrightarrow CO_2 + H_2 \quad (5)$$

As observed, CO is the major product in all cases. The catalytic CO_2 reforming reaction of tars or liquid products [Eq. (1)], CH_4 [Eq. (2)] and C_2H_4 [Eq. (3)] can explained the decrease of these compounds, the increase in H_2 and CO production and the increase in CO_2 conversion when temperature increases. Garcia *et al.* (2001) proposed the participation of the inverse water-gas shift reaction [Eq. (4)] causes the higher CO yield in CO_2 gasification.

For H_2, it can be considered that H_2 production in catalytic CO_2 gasification is mainly due to the catalytic cracking reaction of tars, CH_4 and C_2H_4. The similar trend of H_2 obtained in all cases could indicate the participation of inverse water-gas shift reaction in the CO_2 catalytic gasification.

When consider ethylene as olefins representative. The olefins formation increased with decreasing temperature. This could be suggested that olefins maybe produced from decomposition of cellulose.

$$\text{Cellulose} + \text{heat} \rightarrow CO + H_2 + CO_2 + \text{hydrocarbons} + \text{tar} + \text{char} \qquad (6)$$

When temperature is sufficiently high, the catalyst and gasifying agents react with the products formed in the previous step via several reactions [Eq. (1), (2), and (3)]. Therefore, the olefins formation will be decreased at high temperature.

Ethylene, ethane, and propane were produced more at 600 °C with ZSM-5 catalyst and non-catalytic gasification. Due to the ZSM-5 in this work is commercial catalyst for naphtha cracking process. This suggested that at low gasifying temperature the generated hydrocarbons from cellulose decomposition maybe entered into pore of ZSM-5. The long chain hydrocarbons maybe cracked into ethylene in the pore of ZSM-5. But when temperature increases, more coke deposits in pore and blocked the entering molecule. Therefore, the hydrocarbon molecules cannot enter into pore but it will be reacted with CO_2 via Eq. (1), (2) and (3). As a consequence, lower olefins, higher CO and H_2 in final gas composition.

When consider the effect of catalyst, all catalysts showed only a slight variation. The use of Co and Fe catalysts showed high H_2 content in product gas. This effect was due to the contribution of the water-gas shift reaction [Eq. (5)]. The catalyst transforms liquid products which mainly are tars into gas and modifies the gas composition, increasing H_2 and CO fractions and decreasing CH_4 and C_2+ fractions. The catalytic CO_2 reforming reactions are involved in the final gas composition.

According these results, when compare these results with the work of Encinar *et al.* (1998) in Table 4.5. All gas production from Encinar's work are lesser

than this work. This could be due to the different in biomass source. The bagasse was used as biomass in Encinar's work. However, the trend of gas production in this work is similar to that of Encinar's work.

Table 4.5 Gas production from CO_2 gasification and Encinar's work

Gas production (mol/kg biomass)						
CO_2 gasification of cellulose without catalyst				Encinar *et al.* (1998)		
Temperature (°C)	600	700	800	600	700	800
H_2	1.60	6.62	2.92	0.53	2.66	1.55
CO	6.69	22.08	29.37	1.86	2.37	6.00
CH_4	3.75	3.44	2.64	2.17	1.85	1.31
C_2H_4	1.47	1.30	1.08	0.40	0.18	0.09
C_2H_6	1.52	0.74	0.41	0.20	0.18	0.13

4.3.3 Product Distribution from Steam Gasification

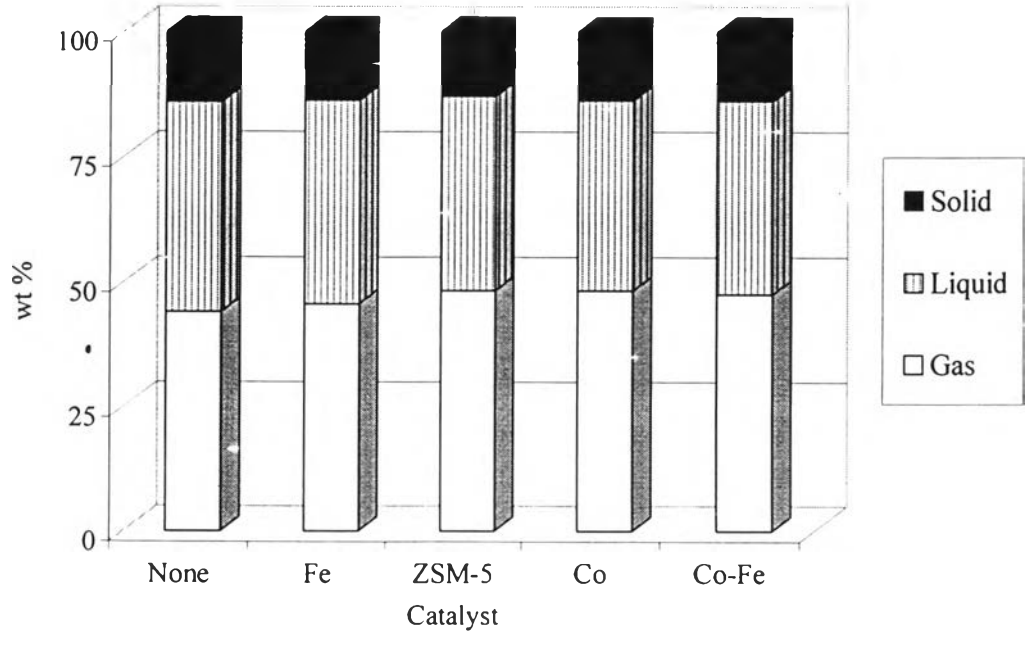

Figure 4.21 Product distribution from steam gasification at 600 °C.

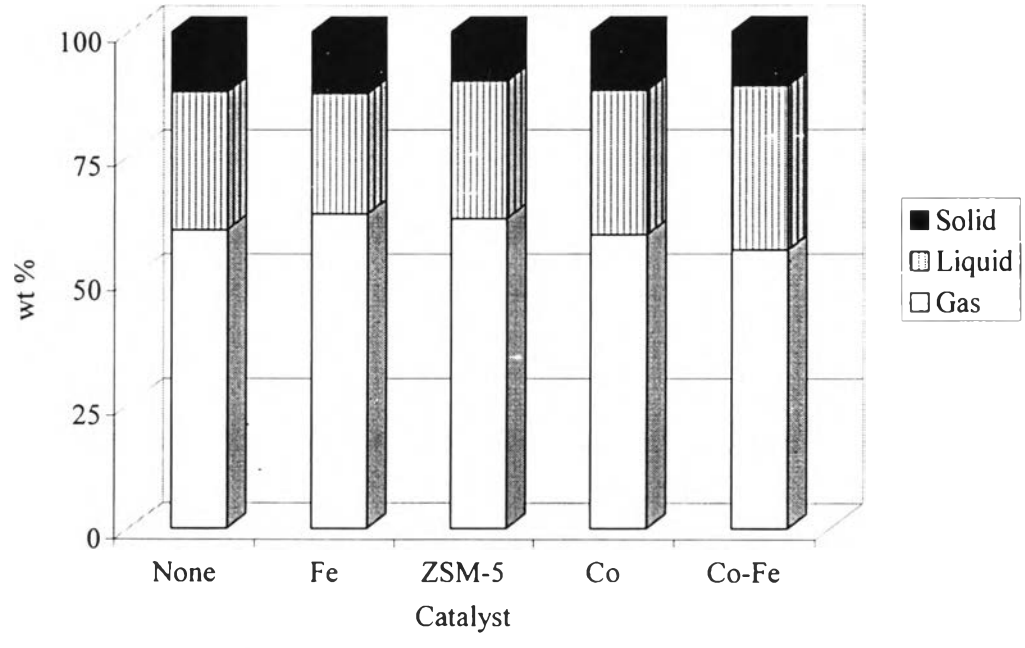

Figure 4.22 Product distribution from steam gasification at 700 °C.

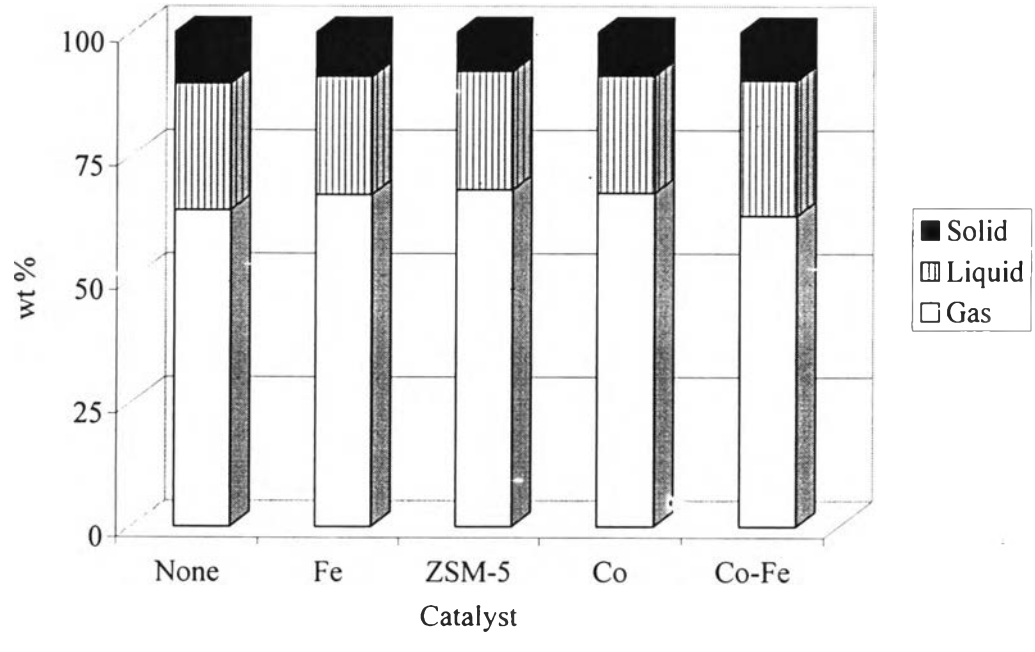

Figure 4.23 Product distribution from steam gasification at 800 °C.

The product distribution of steam gasification at 600, 700, and 800 °C were presented in Figures 4.21, 4.22 and 4.23, respectively. Like CO_2 gasification, an increase in temperature leads to a decrease in solid, liquid yield and an increase in gas yield. This could be also explained by the growing importance of gasification with respect to pyrolysis when temperature increases.

The liquid yield which is obtained from steam gasification was higher than CO_2 gasification. Due to tar reforming was involved from 2 main reactions which are dry reforming [Eq. (1)] and steam reforming [Eq. (7)]. Simell et al. (1997) reported tar reforming with CO_2 was faster than steam reforming and dry reforming was inhibited by the presence of steam.

$$C_nH_x + nCO_2 \rightarrow (x/2)H_2 + 2nCO \quad (1)$$

$$C_nH_x + nH_2O \rightarrow (n+x/2)H_2 + nCO \quad (7)$$

4.3.4 Gas production from Steam Gasification

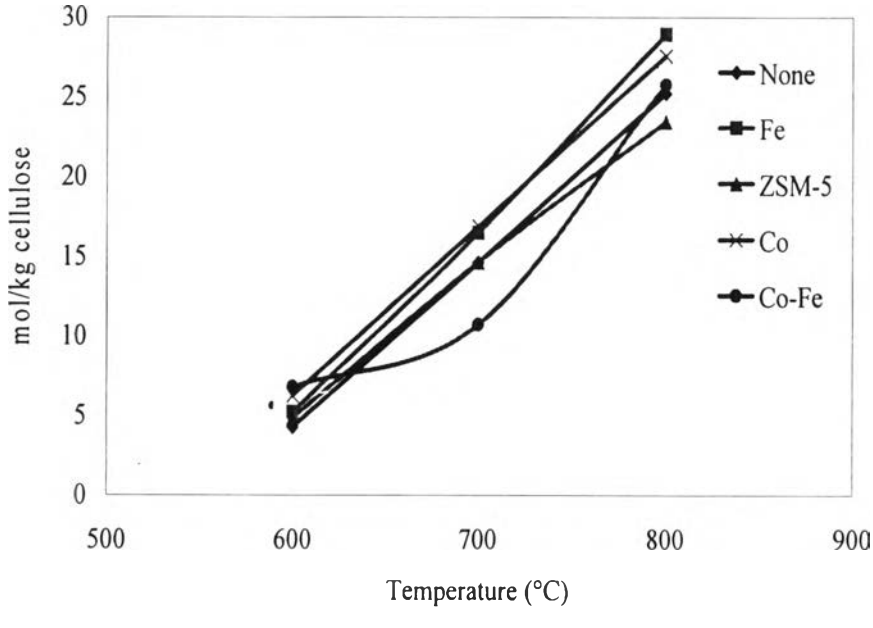

Figure 4.24 H_2 production from steam gasification with and without catalysts : (♦) None, (▲) ZSM-5, (■) Fe, (x) Co, and (●) Co-Fe.

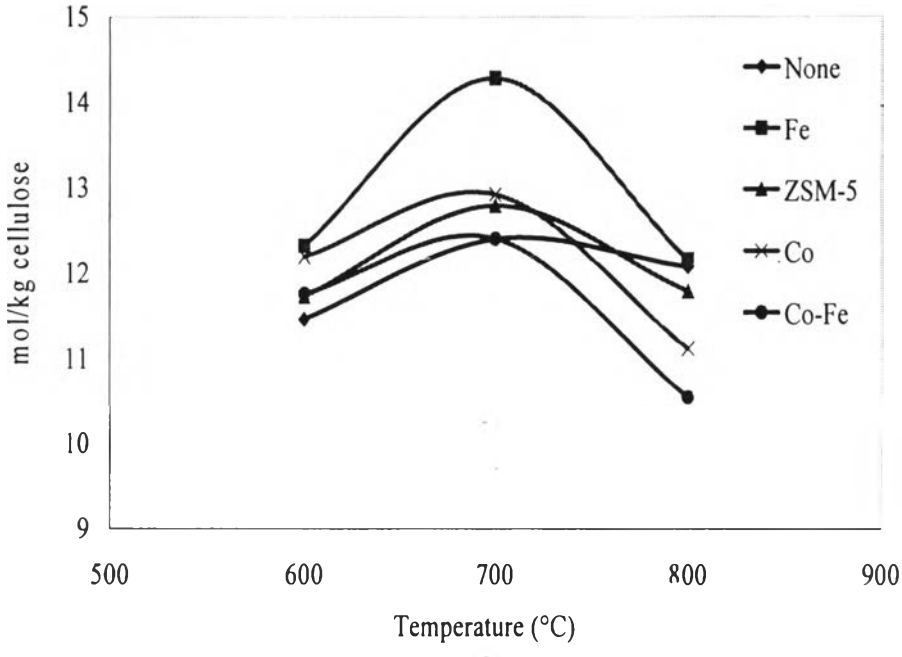

Figure 4.25 CO production from steam gasification with and without catalysts : (♦) None, (▲) ZSM-5, (■) Fe, (x) Co, and (●) Co-Fe.

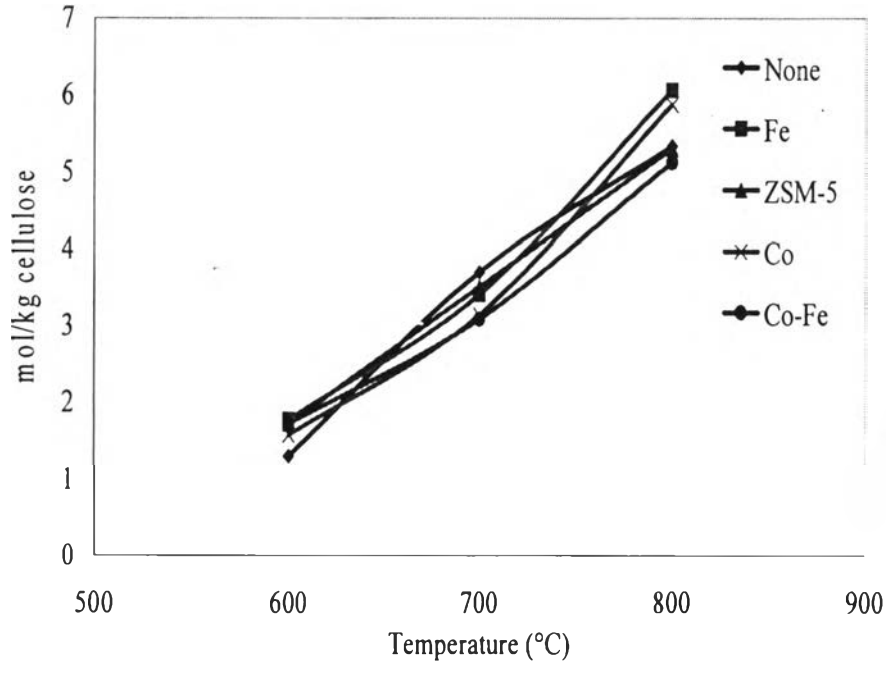

Figure 4.26 CO_2 production from steam gasification with and without catalysts : (♦) None, (▲) ZSM-5, (■) Fe, (x) Co, and (●) Co-Fe.

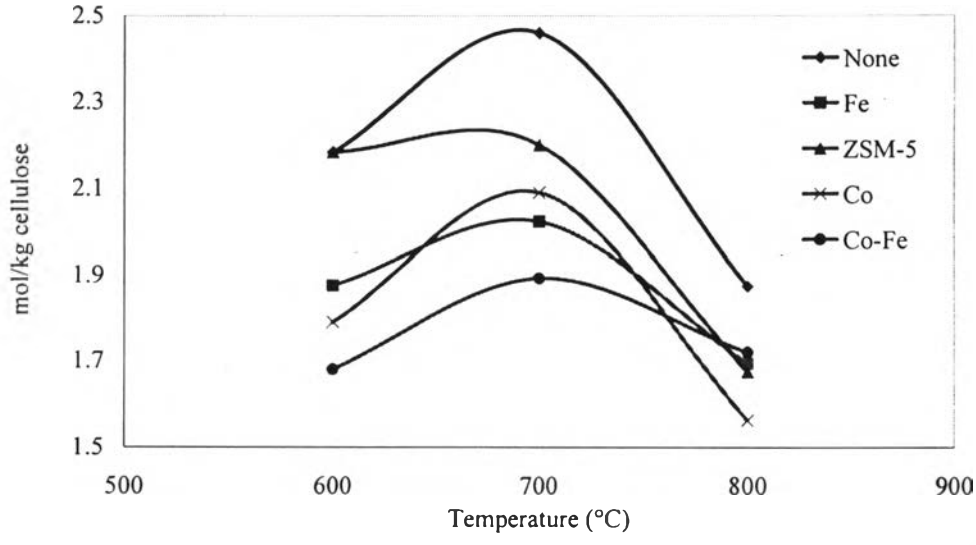

Figure 4.27 CH_4 production from steam gasification with and without catalysts : (♦) None, (▲) ZSM-5, (■) Fe, (x) Co, and (●) Co-Fe.

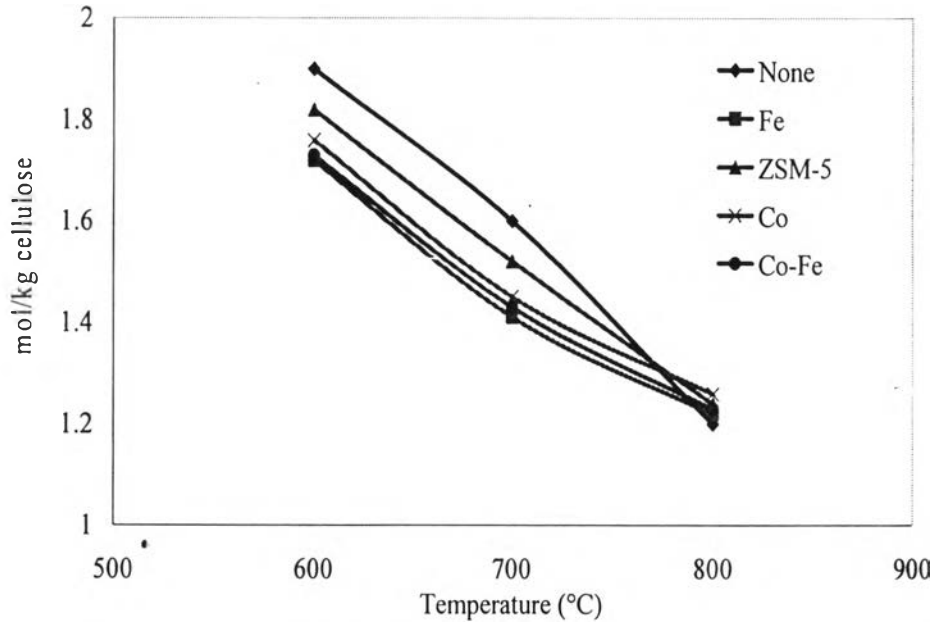

Figure 4.28 C_2H_4 production from steam gasification with and without catalysts : (♦) None, (▲) ZSM-5, (■) Fe, (x) Co, and (●) Co-Fe.

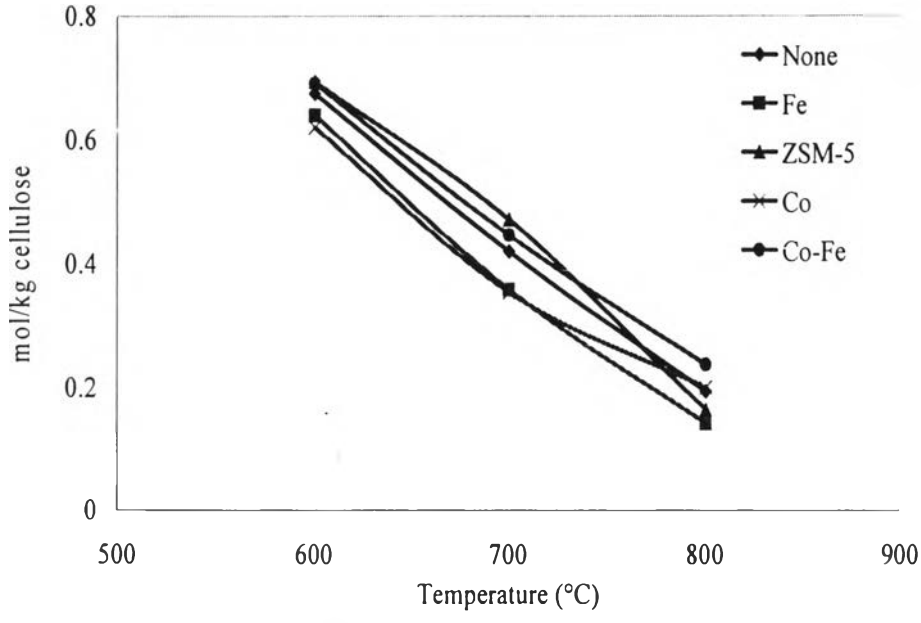

Figure 4.29 C_2H_6 production from steam gasification with and without catalysts : (♦) None, (▲) ZSM-5, (■) Fe, (x) Co, and (●) Co-Fe.

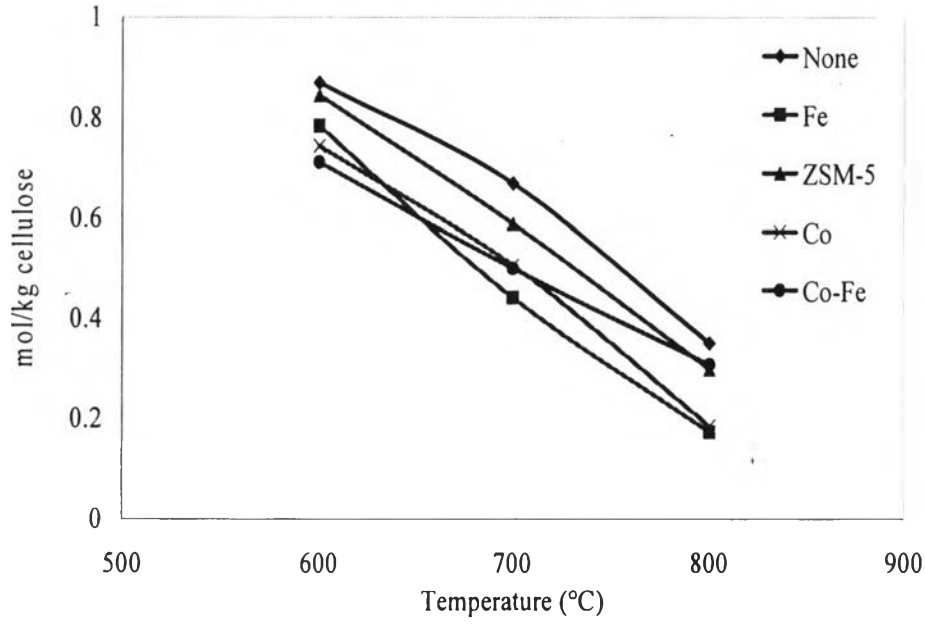

Figure 4.30 C_3H_8 production from steam gasification with and without catalysts : (♦) None, (▲) ZSM-5, (■) Fe, (x) Co, and (●) Co-Fe.

The gas production of H_2, CO, CO_2, CH_4, C_2H_4, C_2H_6, and C_3H_8 are presented in Figures 4.24, 4.25, 4.26, 4.27, 4.28, 4.29 and 4.30, respectively. Like CO_2 gasification, the use of catalyst contribute to the catalytic steam reforming reaction.

$$C_nH_x + nH_2O \rightarrow (n+x/2)H_2 + nCO \quad (7)$$

As observed, H_2 is produced from steam gasification more than CO_2 gasification. This suggested that H_2 was also produced in catalytic steam cracking of tars [Eq. (7)], CH_4 [Eq. (8)] and C_2 [Eq. (9)]. The participation of the water-gas shift reaction [Eq. (5)] causes the generation of higher H_2 yields and lower CO yields in steam gasification than in CO_2 gasification.

$$CH_4 + H_2O \rightarrow 3H_2 + CO \quad (8)$$

$$C_2H_4 + 2H_2O \rightarrow 4H_2 + 2CO \quad (9)$$

$$CO + H_2O \leftrightarrow H_2 + CO_2 \quad (5)$$

$$CO_2 + H_2 \leftrightarrow H_2O + CO \quad (4)$$

Also, the presence of Fe and Co catalyst caused high H_2 content due to the water-gas shift reaction.

At low temperature, methane, ethylene, ethane, and propane maybe produced from pyrolysis or cellulose decomposition. When temperature is sufficiently high, these hydrocarbons will be reformed via several reactions [Eq. (7), (8), and (9)]. Therefore, the formation of hydrocarbons will be decreased at high temperature.

Like CO_2 gasification, it also observed a marked increase in olefins at lower temperature for all cases. The ethylene production is highest in case of non-catalytic gasification. This indicates that the catalyst does not contribute to the olefins formation. It was suggested that under steam or CO_2 atmosphere the catalyst can reduce tar formation and improve H_2 and CO fraction. Olefins maybe produced from pyrolysis or cellulose decomposition but under reactive atmosphere they will be converted into H_2 and CO.

4.4 Liquid Product Characterization

The liquid product obtained from gasification at 700 °C were used as liquid representatives and analyzed by TraceGC/PolarizQ MS (ThermoFinnigan). The capillary column DB-5 MS was used and the compounds were identified by MS (15-500 a.m.u., 70 eV). The qualitative identification of compounds was performed comparing sample mass spectrum with NIST database reference mass spectrum. Figures 4.31, 4.32, 4.33, 4.34, and 4.35 showed the chromatogram of liquid product obtained from gasification without catalyst, Fe, Co, ZSM-5 and Co-Fe, respectively.

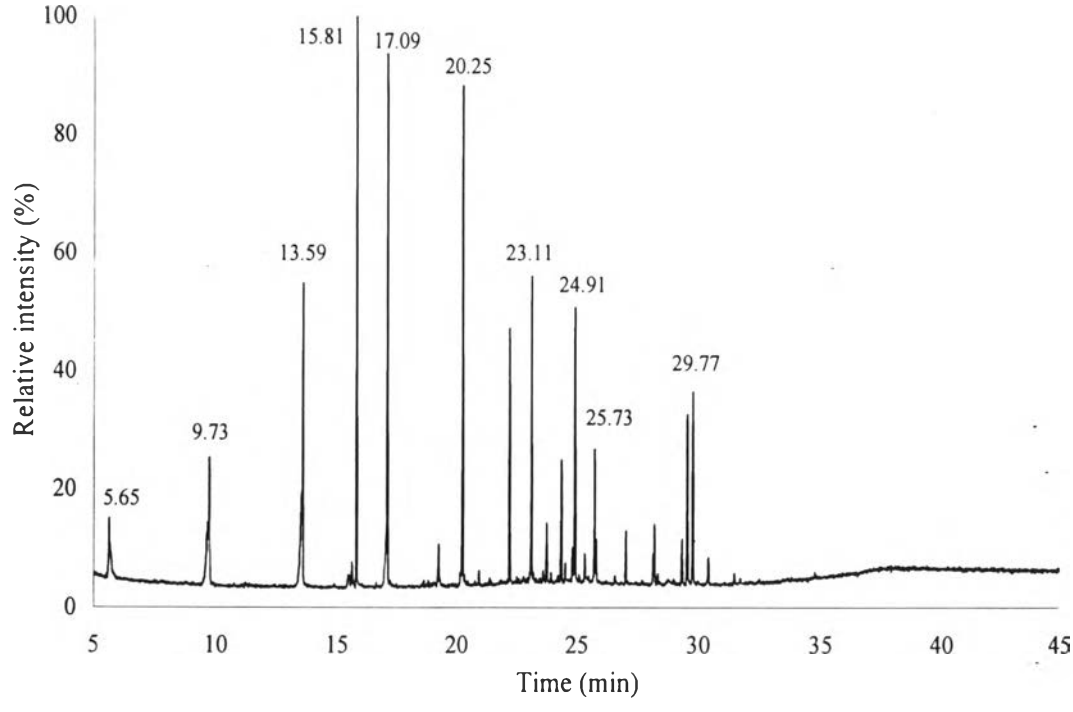

(a)

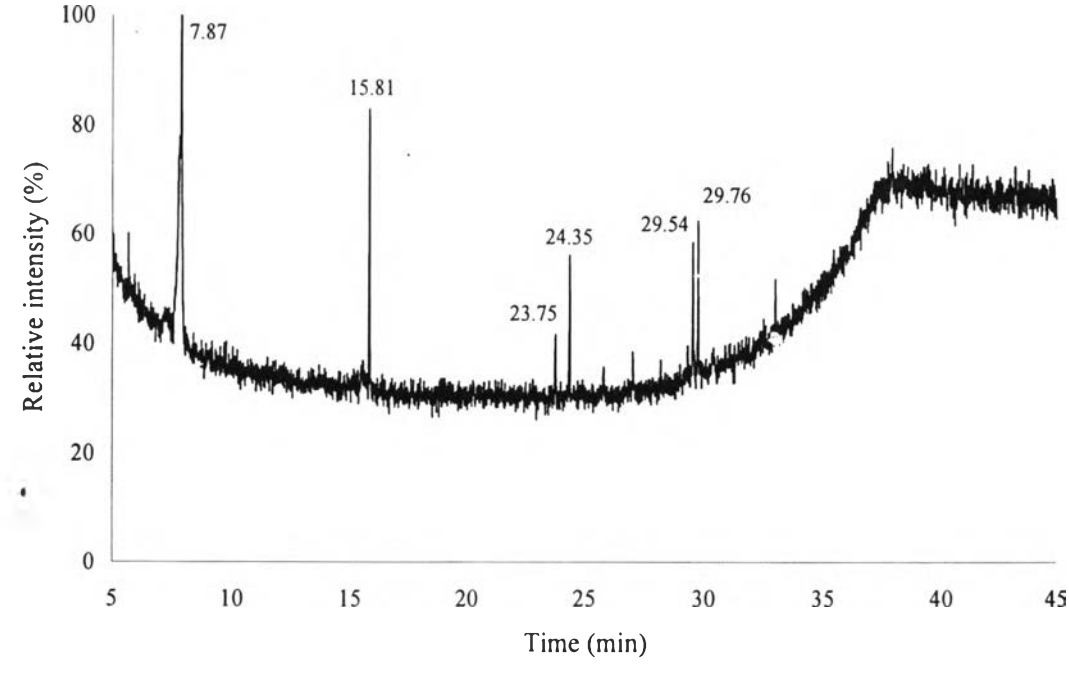

(b)

Figure 4.31 Chromatogram of liquid obtained from CO_2 gasification (a) and steam gasification (b) at 700 °C without catalyst.

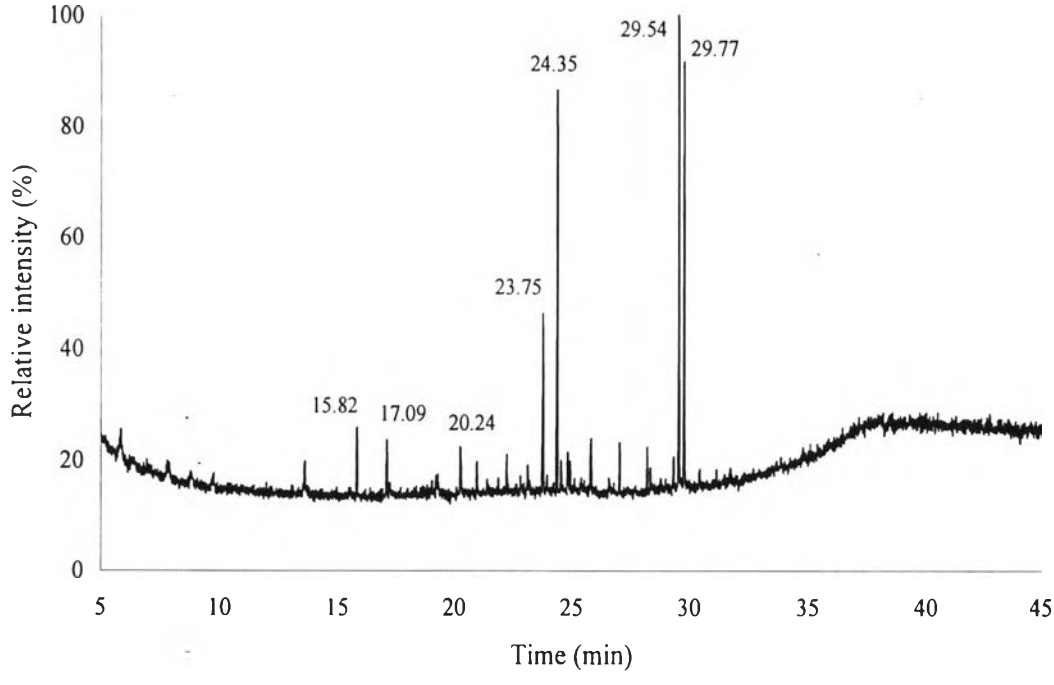

(c)

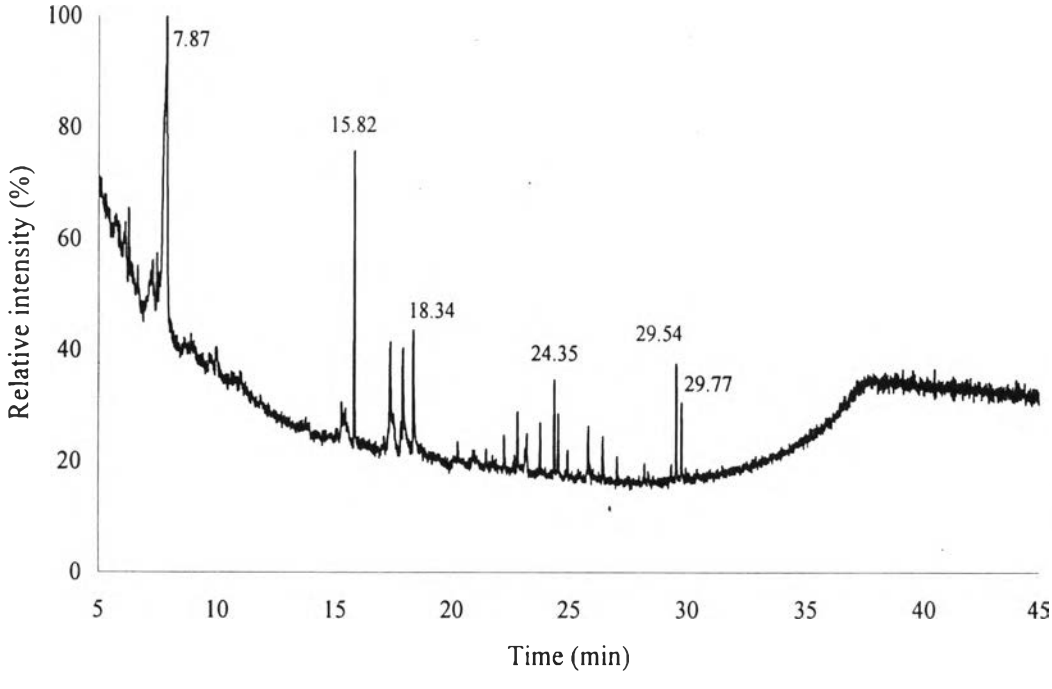

(d)

Figure 4.32 Chromatogram of liquid obtained from CO_2 gasification (c) and steam gasification (d) at 700 °C with Fe catalyst.

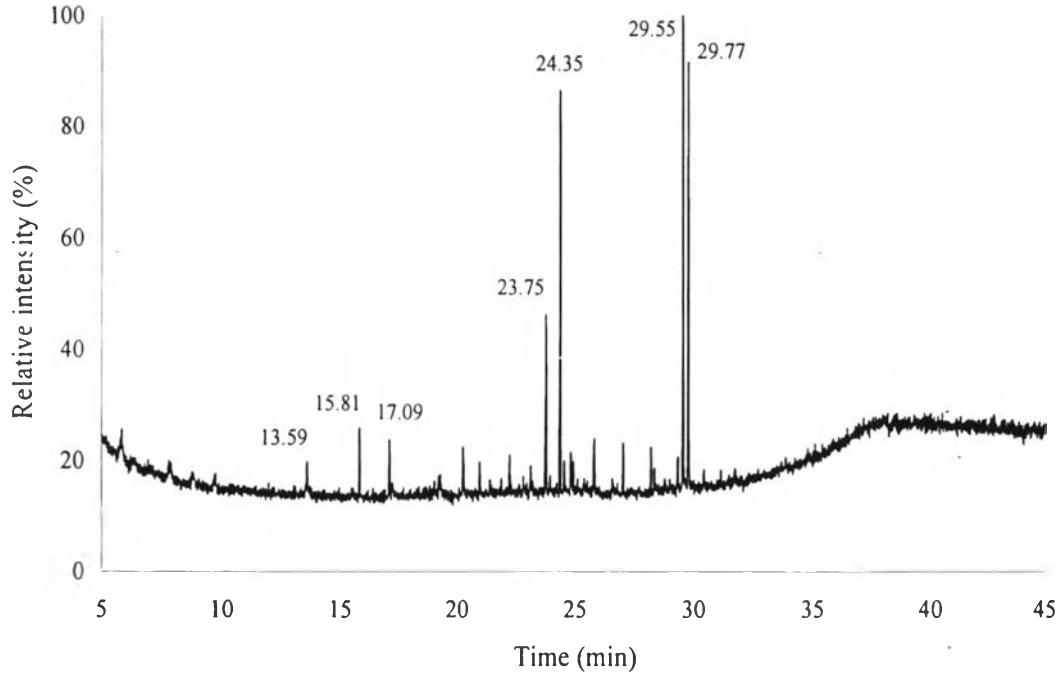

(e)

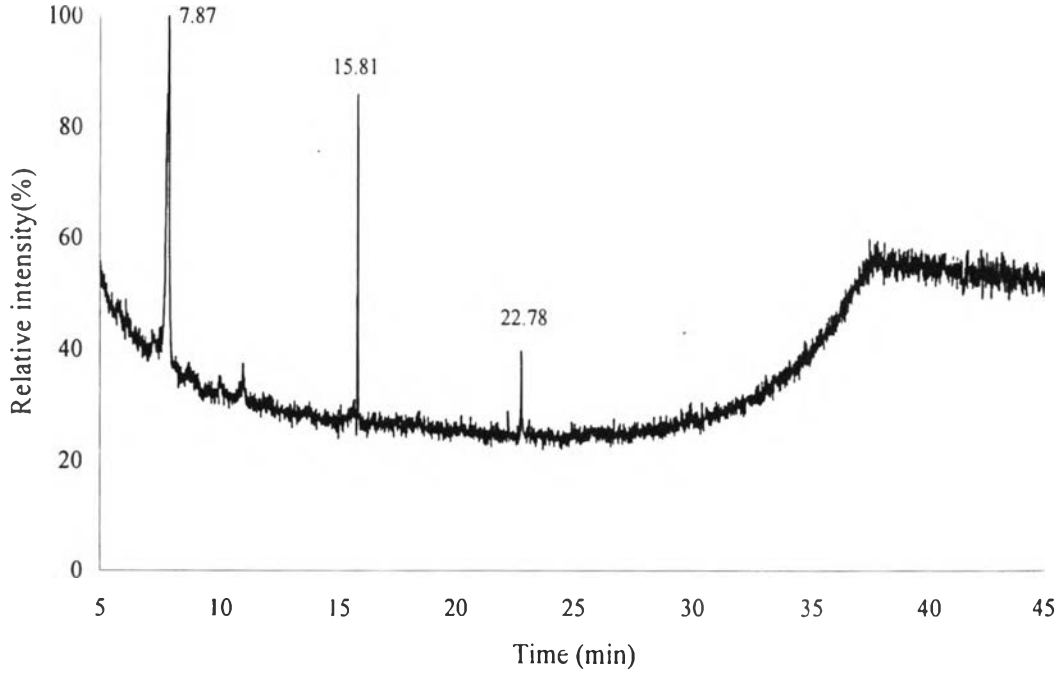

(f)

Figure 4.33 Chromatogram of liquid obtained from CO_2 gasification (e) and steam gasification (f) at 700 °C with Co catalyst.

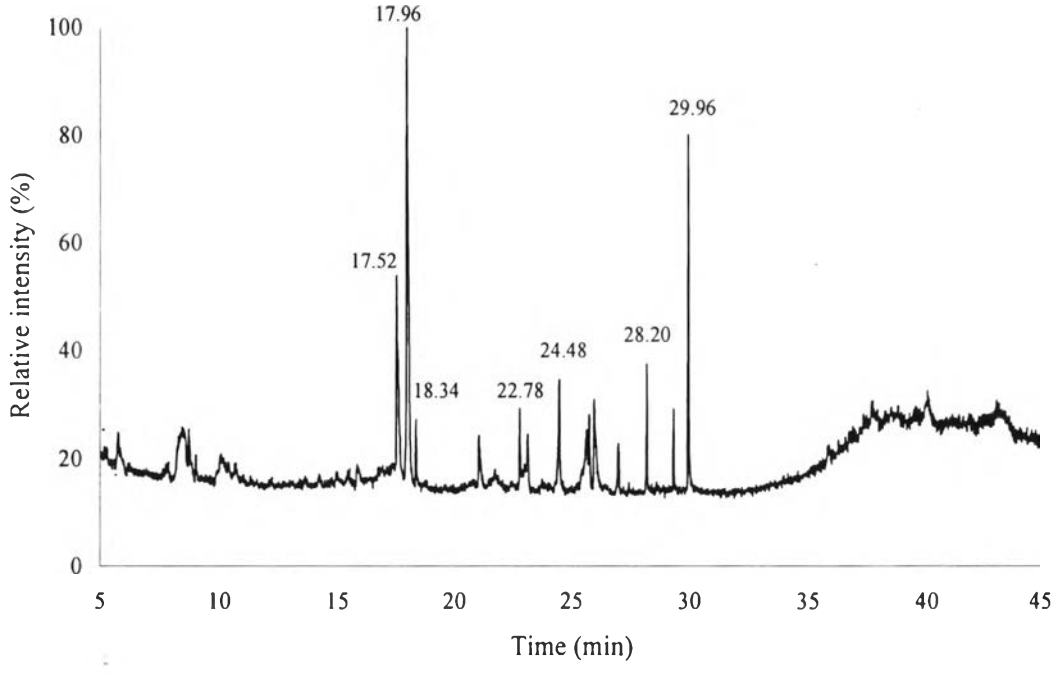

(g)

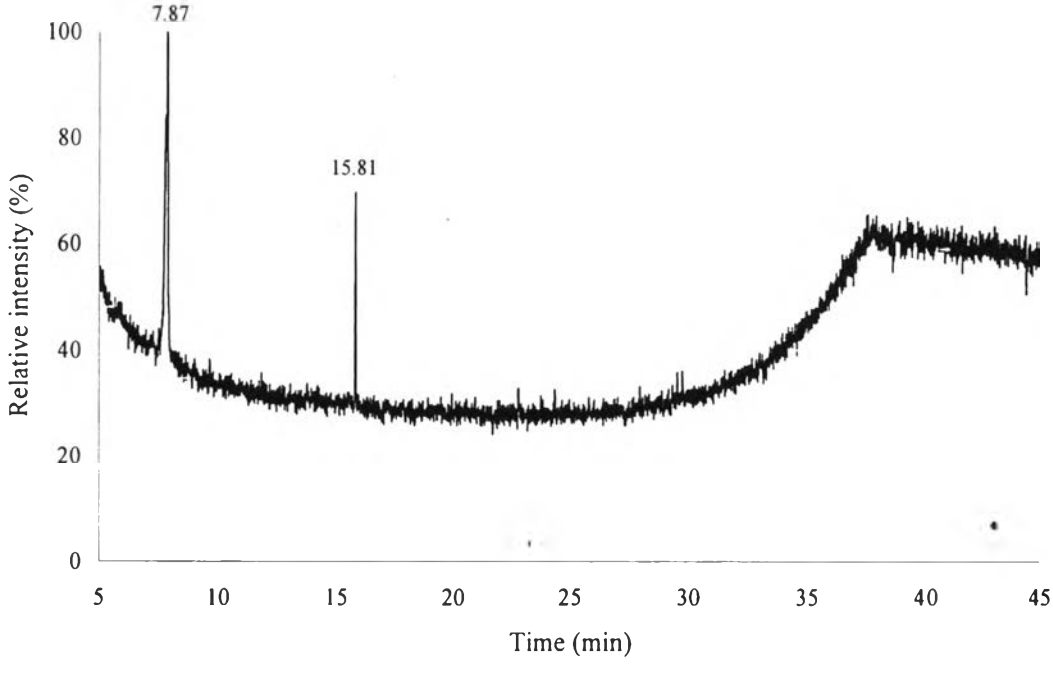

(h)

Figure 4.34 Chromatogram of liquid obtained from CO_2 gasification (g) and steam gasification (h) at 700 °C with ZSM-5 catalyst.

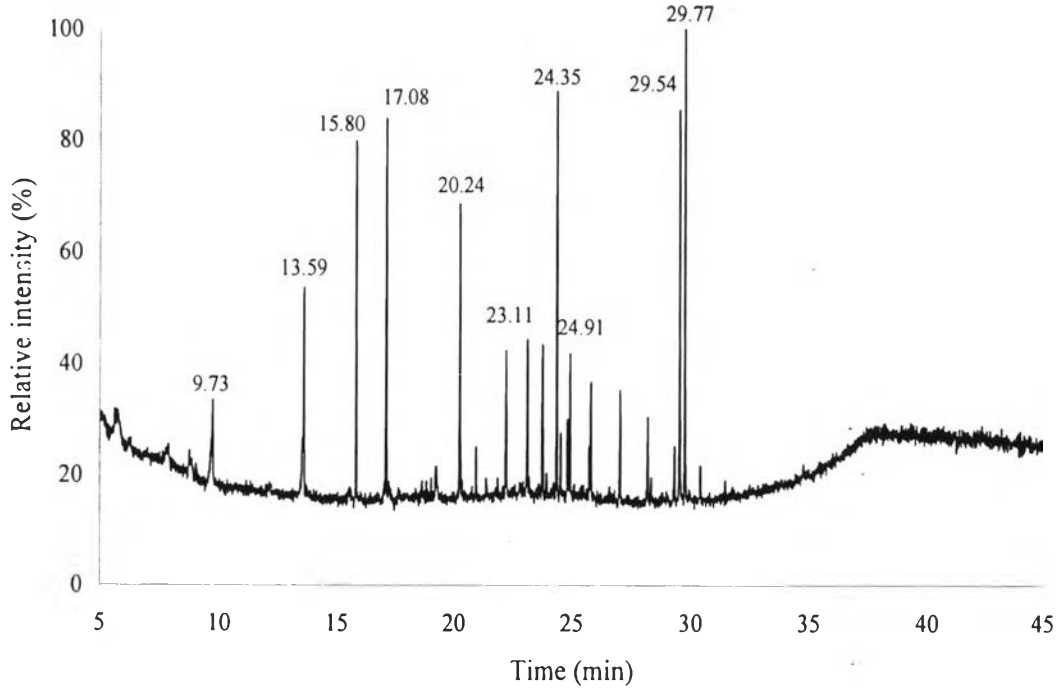

(i)

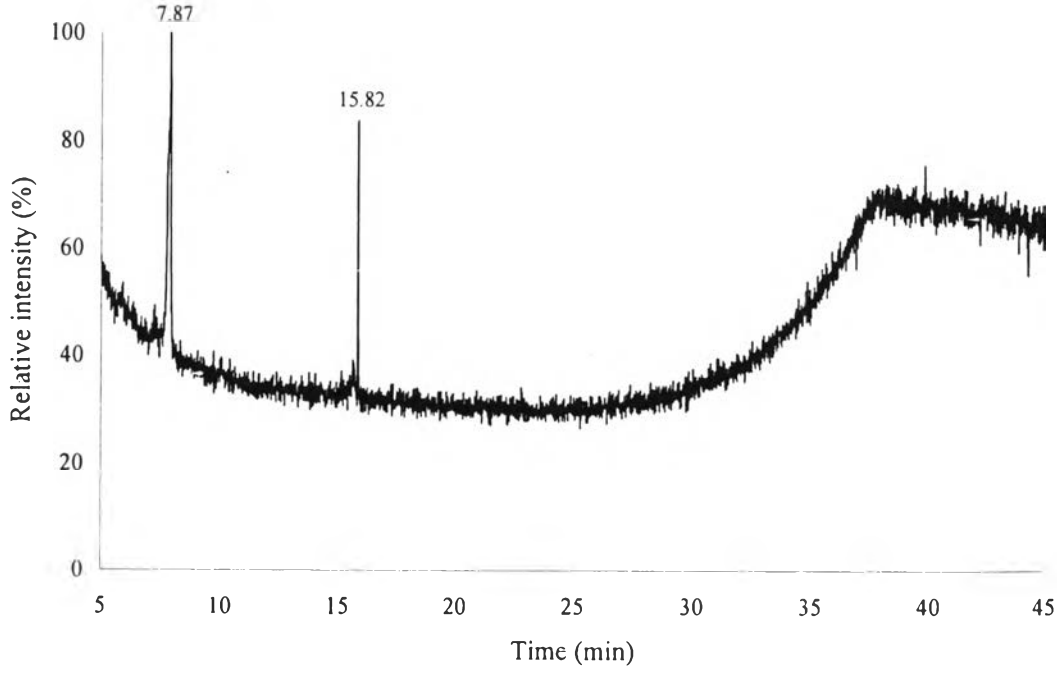

(j)

Figure 4.35 Chromatogram of liquid obtained from CO_2 gasification (i) and steam gasification (j) at 700 °C with Co-Fe catalyst.

Table 4.6 Retention time and possible component of liquid product

Retention Time (min)	Name	Formula	Molecular Weight
7.87	Hexane, 2,2,5,5-tetramethyl	$C_{10}H_{22}$	142
	Hexane, 2,2,3-trimethyl	C_9H_{20}	128
9.73	4-Nonene	C_9H_{18}	126
	Cyclohexane, 1,2,3-trimethyl-,stereoisomer	C_9H_{18}	126
13.59	1,6-Heptadiene,3,3-dimethyl	C_9H_{16}	124
	3-Methyl-hexene	C_7H_{14}	98
15.82	2-Propenylpropanoate	$C_6H_{10}O_2$	114
17.09	2,6-Dimethyl-3-heptene	C_9H_{18}	126
	1,6-Octadiene,5,7,-dimethyl	$C_{10}H_{18}$	138
17.52	Acetylcyclopropane	C_5H_8O	84
	Isopropenylmethylketone	C_5H_8O	84
17.96	Acetic acid anhydride	$C_4H_6O_3$	102
	Isobutenylcarbinol	$C_5H_{10}O$	86
18.34	2-Acetoxyacrylonitrile	$C_5H_5NO_2$	111
	4-Methyl-2-pentylacetate	$C_8H_{16}O_2$	144
20.25	1-Octanol,2-nitro	$C_8H_{17}NO_3$	175
	Nitrocyclohexane	$C_6H_{11}NO_2$	129
22.78	2-Nitroisobutane	$C_4H_9NO_2$	103
23.11	Cyclooctene oxide	$C_8H_{14}O$	126
	2-Octenol	$C_8H_{14}O$	126
23.75	Hexane,2,2-dimethyl-6-phenyl -4. vinyl	$C_{16}H_{24}$	216
	1-Pentene,3,3-dimethyl-5-Phenyl	$C_{13}H_{48}$	174
24.35	THREITOL,2-O-HEPTYL	$C_{11}H_{24}O_4$	220
24.48	Hexadecane	$C_{16}H_{34}$	226
	Tetradecane	$C_{14}H_{30}$	198
24.91	2,3-Dimethyl-3-heptanol	$C_9H_{20}O$	144
	1-Nonen-4-ol	$C_9H_{18}O$	142
25.73	3-Isobutyl-1-methyl-cyclopentanone	$C_{10}H_{18}O$	154
	Cyclopentane,3-isobutyl-1-methyl	$C_{10}H_{20}$	140

Table 4.6 Retention time and possible component of liquid product (continued)

Retention Time (min)	Name	Formula	Molecular Weight
28.2	2-Methyldecane	$C_{11}H_{24}$	156
	2,2,3,3,5,6,6-Heptametylheptane	$C_{14}H_{30}$	198
29.55	4,5-dimethyl-1-[phenylacetyl]imidazole	$C_{13}H_{14}N_2O$	214
29.77	Propanoic acid,2,2-dimethyl-, phenylmethylester	$C_{12}H_{16}O_2$	192
29.96	Tetrahydrofuran 2-[1-methylethyl (1-3,3-dimethyl)	$C_9H_{18}O$	142
	Acrolein, 2-neopentyl	$C_8H_{14}O$	126

Table 4.6 show the retention time of various components and possible component of liquid product. The chromatogram and possible mass from CO_2 and steam gasification at 700 °C with and without catalyst were used as liquid product representative. The results implies that the liquid obtained from gasification mainly consists of the aliphatic and alicyclic compounds, nitrogenated and oxygenated compounds, and small amount of alcohol and aromatic compounds.

The use of catalyst influences in final liquid fraction. The relative intensity of components at retention time ranging from 13-18 minutes are reduced in the case of CO_2 gasification (Figures 4.31 (a) and 4.32 (c)). But in the case of steam gasification, the catalyst does not influence in final liquid fraction. The liquid obtained from CO_2 gasification consist of many kinds of products. This suggested that gasifying agent is strongly affect on the final liquid fraction due to the different of oxidizing ability of gasifying agent. However, quantitative analysis are need to be done in order to have a better understanding of the effect of catalyst and gasifying agent on the gasification mechanism.

4.5 Bio-oil cracking

Based on the results from cellulose gasification with steam and CO_2, the olefins are less produced. On the other hand, CO and H_2 are produced as main products. Therefore, it is difficult to obtain high olefins yield from biomass gasification process in single reactor. However, there are alternative ways for olefins production from biomass which are:

1. Olefins production from biomass-derived oil
2. Olefins production from biomass-derived syngas

Many researches reported that bio-oil from pyrolysis and gasification is composed of many kinds of organic compounds which are in the carbon range C_7-C_{20} (Adjaye and Bakhshi, 1995). These bio-oils have a potential to be used as naphtha substitute. Moreover, bio-oil can be upgraded to value chemicals via catalytic upgrading and steam reforming reaction.

Based on the catalytic bio-oil upgrading, the cellulose was pyrolyzed to obtain bio-oil. Then the catalytic upgrading bio-oil was carried out in the absence of oxygen at 400 and 350°C with ZSM-5 catalyst for 30 minutes.

The bio-oil was fed into tube reactor by syringe pump. The catalyst was placed in the middle of tube reactor and He was fed into reactor in order to purge oxygen.

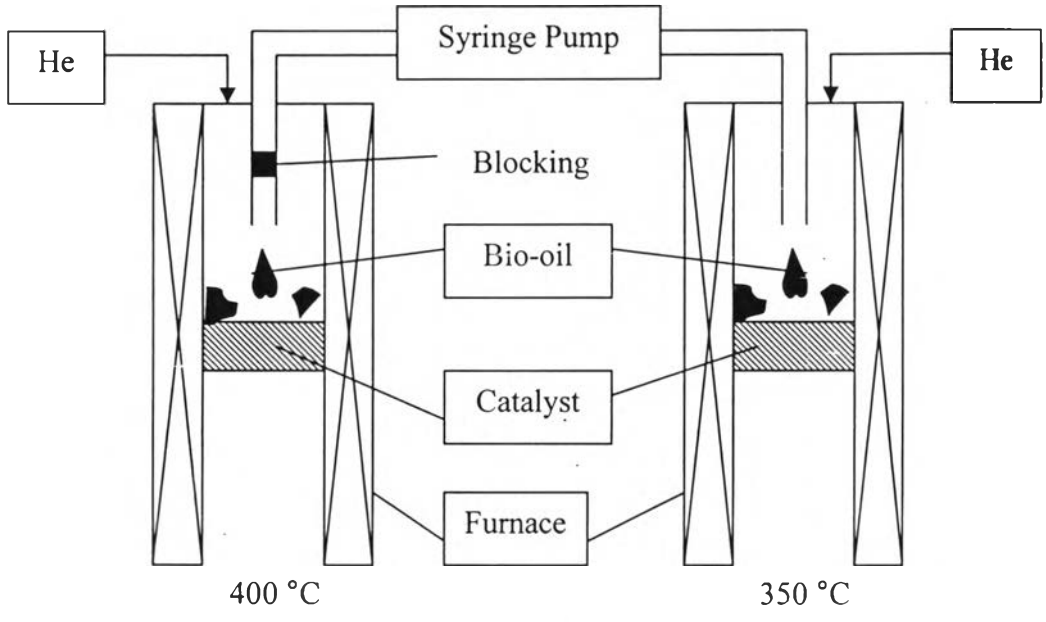

Figure 4.36 Reactor configuration for catalytic bio-oil upgrading.

Table 4.7 Gas composition from catalytic bio-oil upgrading at 350 °C with ZSM-5

Gas composition (mol %)	
CO	60.26
CH_4	0.53
CO_2	39.16

The gas products from catalytic bio-oil upgrading at 350 °C are CO, CO_2 and CH_4. CO is the major fraction of product gas. There are no olefins production. This could be due to the reactor configuration is unsuitable for this process. Because there is coke and gum formation after reaction. During the transportation of bio-oil to the catalyst bed, bio-oil was vaporized and dried by heat from furnace. Then, the resultant bio-oil will be transformed into solid materials such as coke or gum. These coke and gum can block and deposit inside reactor. These solids cause the catalyst deactivation. When increase temperature to 400 °C, the solid formation also appear in reactor.

There is no presence of olefins and other hydrocarbons. This suggested that the coke formation causes the catalyst deactivation. Besides, over time, the reactivity

of some components in bio-oil leads to formation of larger molecules which can block and accumulate in reactor.

Recently, Ramanathan and Lanny (2005) studied the renewable olefins from biodiesel by autothermal reforming. It was found that the short-chain olefins selectivities obtained from biodiesel are only around 40 %. When compare chemical structure of biodiesel with bio-oil, there are many components of bio-oil likely biodiesel components. Therefore, it is also believed that the bio-oil is possible to convert into olefins by autothermal reforming.

4.6 Fischer-Tropsch Synthesis

Another possible way to produce olefins from biomass is olefins production from biomass-derived syngas. It is generally known that CO and H_2 are main products from gasification process, and the gas which is a mixture between CO and H_2 is called synthesis gas. This syngas can be used to produce olefins through the so-called Fischer-Tropsch Synthesis process. Currently, the process of synthesizing hydrocarbon products from syngas has been developed as an industrial process. For example, Sasol plant in South Africa has successfully produced syngas from coal by using Co and Fe as catalyst.

Main reaction :	$CO + 2H_2 \rightarrow [- CH_2 -] + H_2O$	(10)
Methane :	$CO + 3H_2 \rightarrow CH_4 + H_2O$	(11)
Olefins :	$nCO + (2n)H_2 \rightarrow C_nH_{2n} + nH_2O$	(12)
Paraffins :	$nCO + (2n+1)H_2 \rightarrow C_nH_{2n2} + nH_2O$	(13)
Alcohol :	$nCO + 2nH_2 \rightarrow C_nH_{2n+1}OH + (n+1)H_2O$	(14)

Based on the above fact, the Fischer-Tropsch synthesis process was simulated and the catalyst is the same as that used in the gasification experiment. Also, the ratio of H_2 to CO is the same as that mentioned in the theory ($H_2/CO = 2$) and the temperature for the experiment is set at 350 °C.

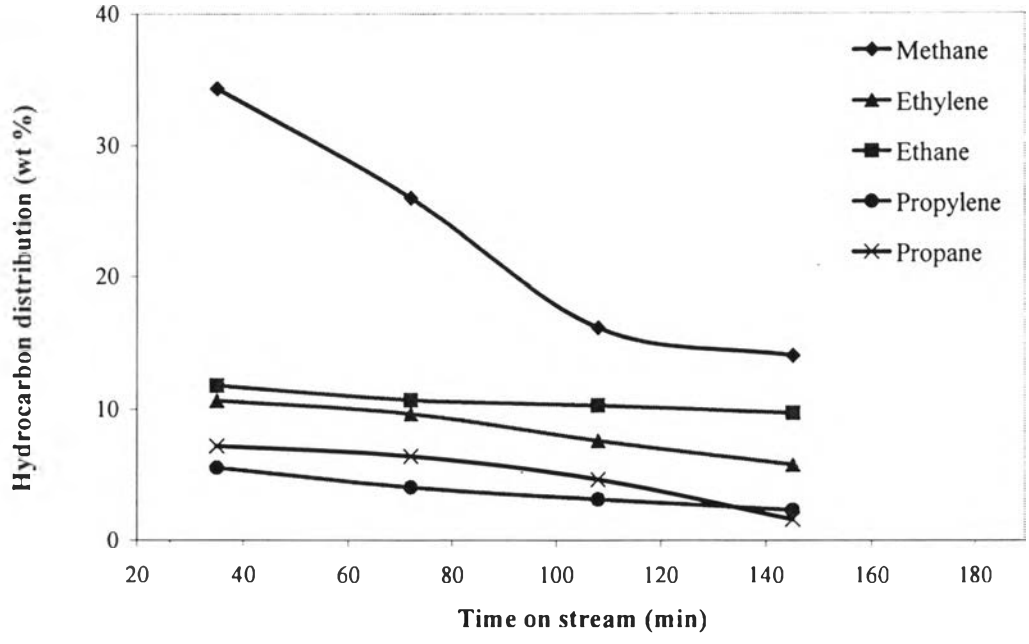

Figure 4.37 Hydrocarbon distribution from Fischer-Tropsch synthesis at 350 °C with Fe catalyst.

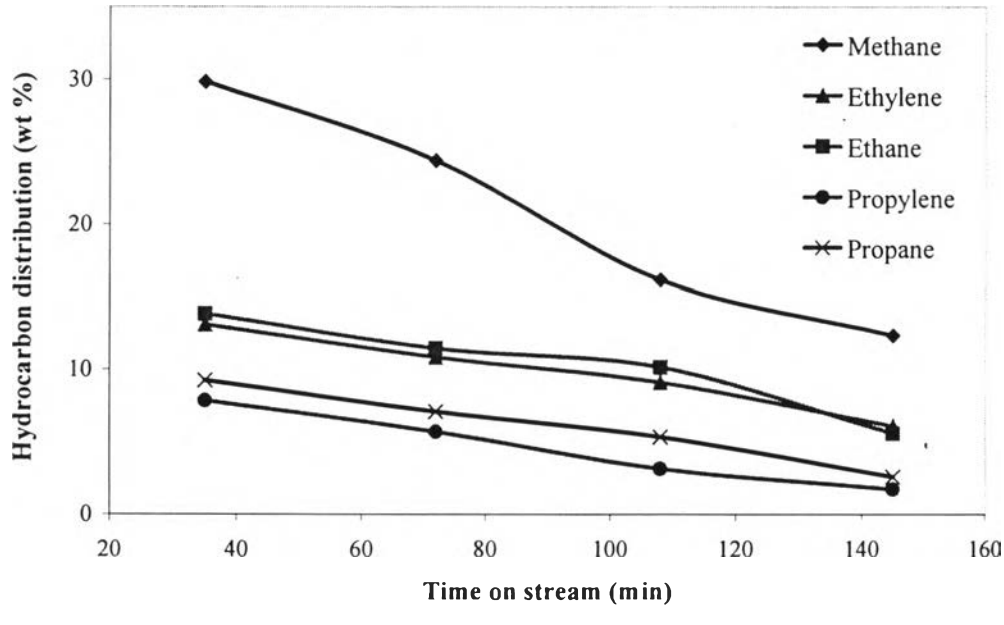

Figure 4.38 Hydrocarbon distribution from Fischer-Tropsch synthesis at 350 °C with Co catalyst.

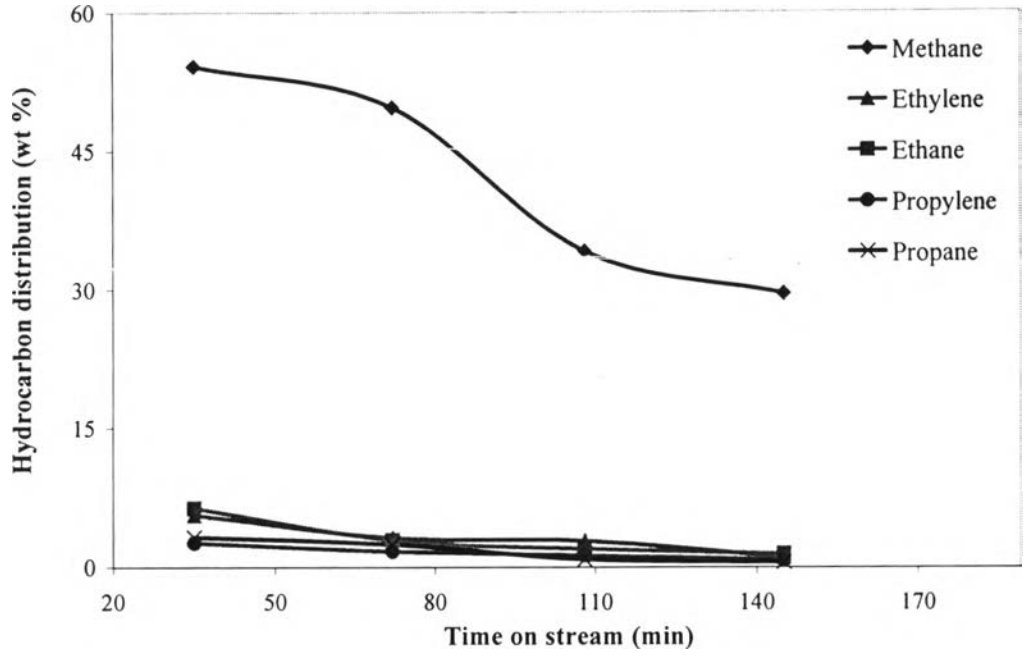

Figure 4.39 Hydrocarbon distribution from Fischer-Tropsch synthesis at 350 °C with ZSM-5 catalyst.

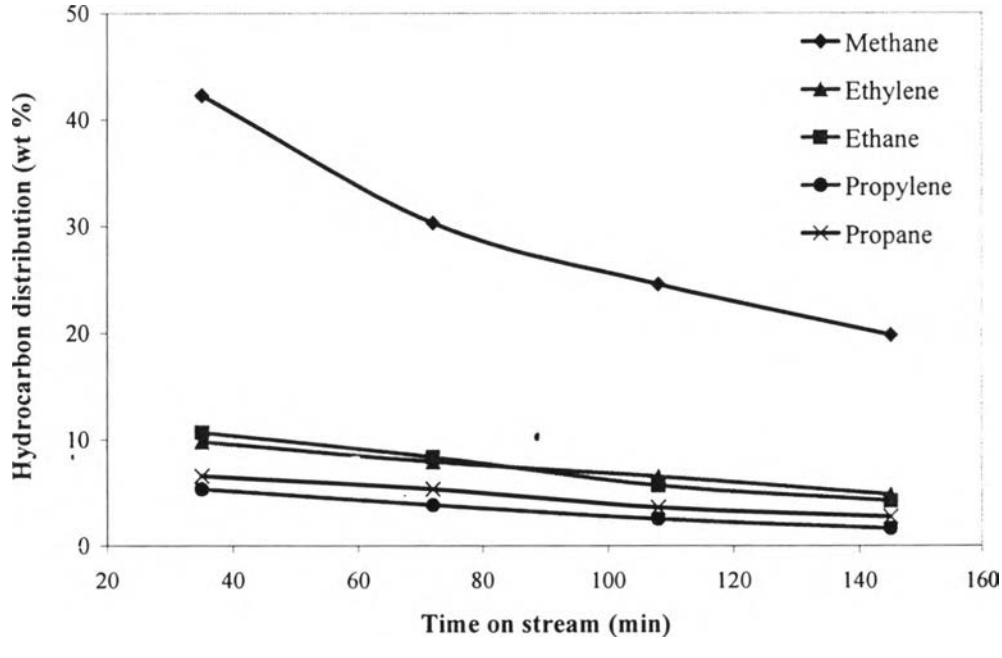

Figure 4.40 Hydrocarbon distribution from Fischer-Tropsch synthesis at 350 °C with Co-Fe catalyst.

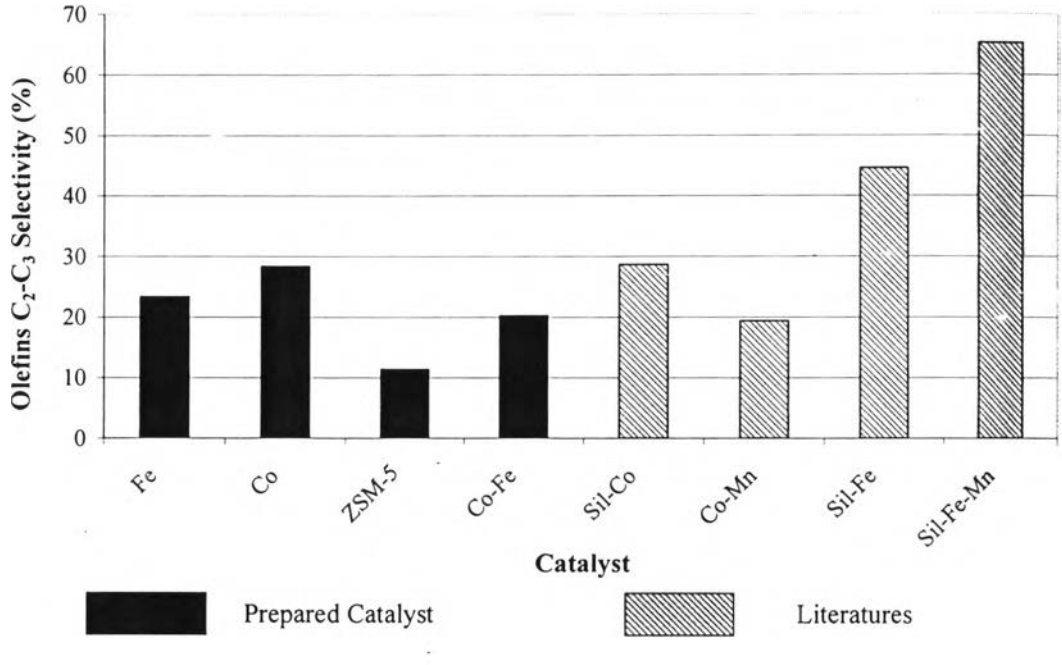

Figure 4.41 Comparison between prepared catalyst and catalysts in literatures.

The results showed that hydrocarbons which were produced in this process include methane, ethylene, ethane, propylene, and propane. It is possible that other hydrocarbon products are produced in this process, but they cannot be traced or measured by the Column used in GC. Because the Column (CarbonPlot) can measure hydrocarbons only in the carbon range between C_1-C_3.

The amount of hydrocarbon was highest at the beginning of the process, and the amount gradually reduced according to the time elapses due to the deactivation of catalyst. The yields of ethylene and propylene are highest when Co is used as catalyst (ethylene = 13.1 wt%, propylene = 7.8 wt%). The comparison of olefins selectivity value from the catalyst used in this study and those of other studies in which different catalysts were used reveal that the olefins selectivity value in this study is relative low, at approximately 28.35%. This low olefins selectivity value may result from the fact that the catalyst used in this experiment is a basic metal whose attributes have not been upgraded or improved. Also, neither promoter nor support were used.